Angewandte Chemie
Eine Zeitschrift der Gesellschaft Deutscher Chemiker

Supporting Information

High-Throughput Optimization of Photochemical Reactions using Segmented-Flow Nanoelectrospray-Ionization Mass Spectrometry

A. C. Sun, D. J. Steyer, R. I. Robinson, C. Ginsburg-Moraff, S. Plummer, J. Gao, J. W. Tucker, D. Alpers, C. R. J. Stephenson, R. T. Kennedy**

Supplementary Material

This PDF file includes:

Materials and Methods

Figures S1 to S19

Tables S1 to S3

References 64 to 68

Table of Contents

Materials and Instrumentation

Chemicals were either used as received or purified according to the procedures outlined in *Purification of Common Laboratory Chemicals*. Perfluorodecalin (PFD) and trichloro(1*H*,1*H*,2*H*,2*H*-perfluorooctyl)silane were purchased from Oakwood Products (Estill, SC). All other reagents were purchased from Fisher Scientific or Sigma Aldrich. Hygroscopic *N*-oxide substrates were dried on a high vacuum line for 6 h at ambient temperature prior to use. Pyridine N-oxide was dried on a high vacuum line at 60 °C for 12 hours. Thin-layer chromatography (TLC) analysis of reaction mixtures was performed using Merck silica gel 60 F254 TLC plates and visualized by a dual short wave/long wave UV lamp. Column flash chromatography was performed using 230–400 mesh silica gel or automatically by a Biotage Isolera Four, with Biotage SNAP KP-Sil 25 or 50 g flash chromatography cartridges. Mass-directed purification was performed with an Agilent high performance liquid chromatography/mass spectrometry (HPLC/MS) auto purification system using electrospray ionization (ESI), positive ion mode.

nESI-MS analysis of droplet samples was performed on an Micromass Quattro Ultima triple quadrupole mass spectrometer (Waters, Milford, MA). Nuclear magnetic resonance (NMR) spectra were recorded using an internal deuterium lock on Varian MR400, Varian Inova 500 and Varian VNMRs 700 spectrometers, and Bruker Advance 600. Chemical shifts for ^{1}HNMR were reported as δ, parts per million, relative to the signal of $CHCl_3$ at 7.26 ppm or DMSO-d6 at 2.50 ppm. Chemical shifts for ^{13}CNMR were reported as δ, parts per million, relative to the center line signal of the $CDCl_3$ triplet at 77.36 ppm. Multiplicities are reported using the following abbreviations: s = singlet, d = doublet, t = triplet, q = quartet, quint = quintet, m = multiplet, br = broad resonance, dd = doublet of doublet, dt = doublet of triplet, etc. High-resolution mass spectra (HRMS) for compound characterization were recorded at the Mass Spectrometry Facility at the Department of Chemistry of the University of Michigan in Ann Arbor, MI, on a Micromass AutoSpec Ultima Magnetic Sector mass spectrometer using ESI, positive ion mode. IR spectra were recorded on a Perkin-Elmer Spectrum BX FT-IR spectrometer fitted with an ATR accessory.

LED and heat sink parts for our 25 Cree LED array photoreactor were purchased from LED Supply (https://ledsupply.com) with the following item codes: CREEXTE-ROY-X (XLamp XT-E Royal Blue LEDs), MAKERSLED (MakersLED Heat Sink), PDA060B-XXXB (60W Phihong IP67 Constant Current AC Drivers). A Westpointe Electrical Co Wp 4'' Hi Velocity Fan 1002 Personal Fan was purchased from http://amazon.com.

Photoreactor Setup Design

At the onset of our studies, our first objective was to identify a modular photoreactor to enable well plate-based photocatalytic reactions. While there are several commercially available systems designed for photochemical parallel synthesis, we recognized that there were significant limitations associated with each platform (**Figure S1**). The configurations of SynLED (Millipore-Sigma) and Kessil lamps (Kessil) were demonstrated to be more compatible with vial-based reaction screens. The Lumidox setup (Analytical Sales) can accommodate the dimensions of a standard well plate while allowing for the use of a stir plate to promote mixing; however, we were concerned about the low intensity of the LEDs (14 mW LED max output) relative to other common light sources.

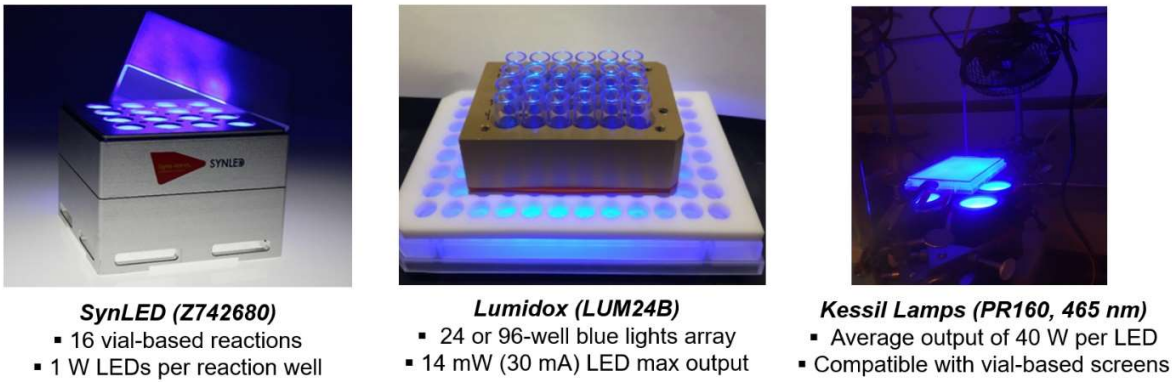

Figure S1. Commercially available photoreactors for parallel synthesis. (Left) SynLED photoreactor setup. (Middle) Lumidox photoreactor system. (Right) Kessil lamp screen setup.

As such, we aimed to design a customized photoreactor with the following features: (1) high photon flux to enable reaction acceleration, (2) successful interface with commercially available well plates, and (3) a modular, low footprint design for facile use on the benchtop. With these considerations in mind, we assembled a 25 LED array of Cree Royal Blue XTE LEDs (2 W per LED, 50 W total output) (**Figure S2, S3**).

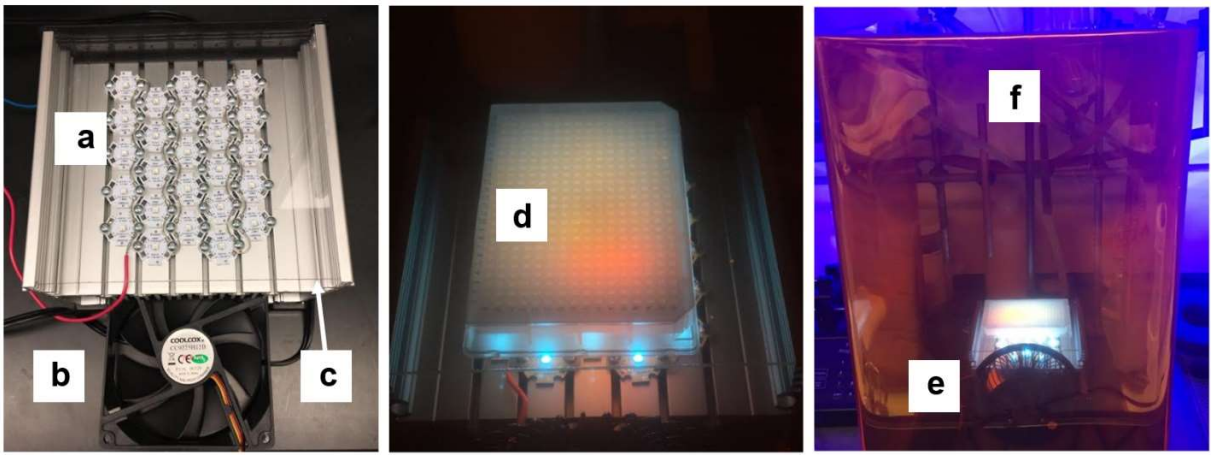

Figure S2. (Left) Cree Royal Blue XT-E LED photoreactor setup with (a) 25 array of Cree LEDs, (b) fan positioned underneath heat sink, (c) acrylic shield. (Middle) Close-up view of irradiation device in operation with (d) 384 multiwell plate containing reaction samples. (Right) Entire setup for irradiation of in-droplet perfluoroalkylation reactions with (e) fan positioned adjacent to heat sink and (f) amber protective shield.

The LEDs were mounted onto a heat sink (MakersLED heat sink, LED Supply), with two fans placed below and adjacent to the heat sink, to provide sufficient cooling to maintain reactions at ambient temperatures. Reaction internal temperatures were recorded to be between 35 – 40 degrees Celsius across the course of a 1 h reaction. An acrylic shield positioned 5 cm above the LED array provided a mounting stage for the reactor tubing, as well as an additional layer of protection for the LEDs. A custom-built plastic amber light shield (built by Ann Arbor Plastics, Saline, MI) was placed around the setup for user eye protection.

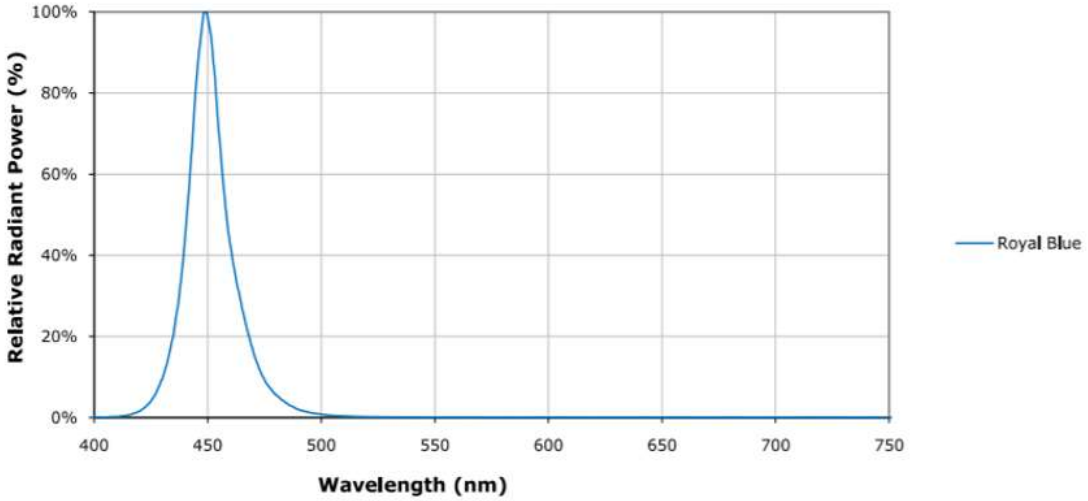

Figure S3. Relative spectral power distribution for a single Cree Royal Blue LED. Source: https://www.ledsupply.com/content/pdf/leds-cree-xte_documentation.pdf

To determine light intensity variance across a 384 well plate positioned on our photoreactor, we obtained absorbance measurements to detect formation of a phenanthroline-bound Fe(II) complex using a ferrioxalate actinometer (**Figure S4**). It is noteworthy that absorbance intensity corresponds with moles of phenanthroline-bound iron complexes formed. Since photon flux is inversely proportional to absorbance (Equation 1), we reasoned that variances in absorbance would be reflective of photon flux differences across the well plate.

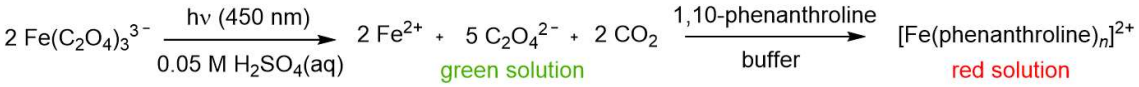

Figure S4. Ferrioxalate actinometer reaction scheme.

$$\text{Photon Flux} = \frac{\text{mol actinometer}}{(\phi) \times (t) \times (f)} \qquad (1)$$

ϕ = quantum yield of actinometer
t = reaction time
f = fraction of light absorbed
at wavelength of light source ($1 - 10^{-A}$)

As such, we performed identical actinometry experiments in each well using our photoreactor. This experiment closely followed a procedure reported by Cismesia and Yoon.[63] Namely, a 0.15

M solution of ferrioxalate was prepared by dissolving 2.21 g of potassium ferrioxalate hydrate in 30 mL of 0.05 M H_2SO_4. A buffered solution of phenanthroline was prepared by dissolving 50 mg of phenanthroline and 11.25 g of sodium acetate in 50 mL of 0.5 M H_2SO_4. Both solutions were stored in the dark. To determine light intensity differences across the 384 well plate, 40 µL of the ferrioxalate solution was deposited into each well using a multichannel pipette and irradiated for 90.0 seconds. After irradiation, 1 µL of the phenanthroline solution was added to each well. The solution was then allowed to rest for 1 h to allow the ferrous ions to completely coordinate to the phenanthroline. The absorbance of the solutions across the plate was measured at 436 nm using a Perkin Elmer EnVision Multimode Plate Reader (**Figure S5**). Based on our absorbance measurements, we were seeing consistent absorbance levels across the plate, which suggests that any potential light intensity variance did not seem to affect the outcome of reactivity.

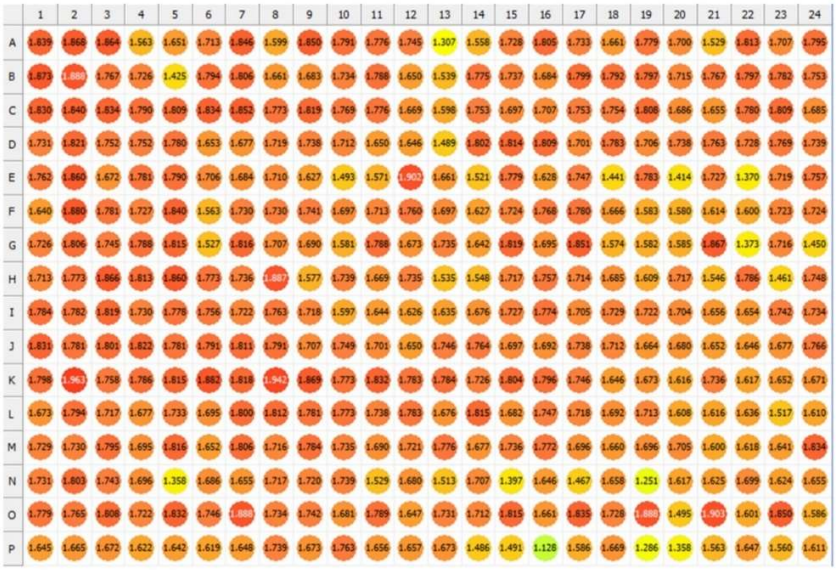

Figure S5. UV-vis absorbance measurements performed for actinometry experiments. UV-vis measurements were obtained at a wavelength of 436 nm. The above heat map was generated using a logarithmic scale of 2.28 based on absorbance units.

(64) Cismesia, M.; Yoon, T. *Chem. Sci.* **2015**, *6*, 5426-5434.

General Perfluoroalkylation Reaction Setup for 2 µmol Well Plate Screens

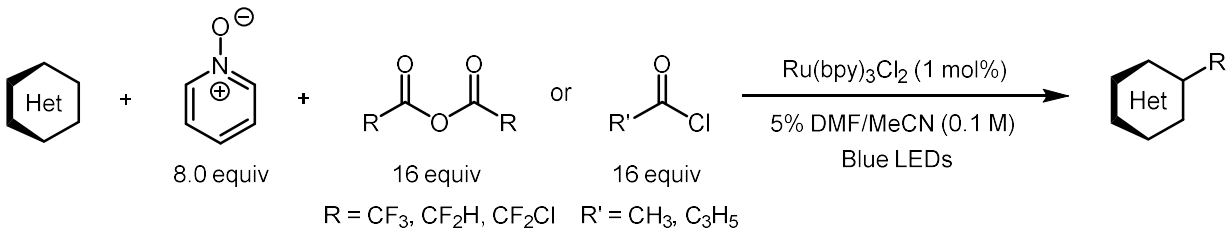

Photocatalyst (1 mol%), pyridine N-oxide (8 equiv), and 5% DMF/acetonitrile (0.2 M) were added to a vial charged with a stir bar. The solution was sparged with a stream of nitrogen gas for 5 min. Acetic anhydride (16 equiv) was subsequently added, and the solution was stirred for 10 min to facilitate formation of the acylated species. Separate solutions of substrate in 5% DMF/acetonitrile (0.2 M) were also prepared. 10 µL of each solution were combined in a 384 well plate to form the final reaction solution. Reactions were irradiated using the photoreactor setup described above without mixing.

Droplet Generation Method

Droplet generation from microwell plates (MWPs) was performed using equipment and methods described previously (*13c, 23*). Before generation, all samples were subjected to a dilution of 500:1 by a 50:50 methanol:water solution w/0.5% formic acid, with the exception of the trifluoromethylation condition screen (see SI pg.S16), in which samples were diluted down to an additional 4:1 with acetonitrile. Samples were drawn into either 100 µm or 150 µm inner diameter (i.d) x 360 µm outer diameter (o.d.) perfluoroalkoxyalkane (PFA) tubing (IDEX Health and Science, Oak Harbor, WA) by a PHD 2000 Programmable syringe pump (Harvard Apparatus,

Holliston, TX). A 25 µL glass syringe (Hamilton, 1700 Series Gastight Syringe, N Termination, Part No. 80285) filled with PFD and connected to a reducing union, 1/16'' to 360 µm (Valco Instruments Co., Houston, TX, Part No. C360TU1PK6) and ferrule (Valco Instruments Co., Houston TX, Part No. C360NFPK) was mounted onto the syringe pump. 8 µL samples were deposited into 384 PCR MWPs (Corning, Corning, NY) covered with a layer of PFD. While solution was being withdrawn through the tubing, an XYZ-position manipulator moved the tubing between sample wells and fluorous phase to form alternating droplet/carrier phase trains (**Figure S6**). When diluted only with methanol:water diluent, 8 nL droplets with 12 nL perfluorodecalin spacing were generated at 800 nL/min, except otherwise stated. When additional acetonitrile dilution was performed, droplets were found to be less stable. As such, 6 nL droplets with 10 nL spacing were generated at a flow rate of 600 nL/min .

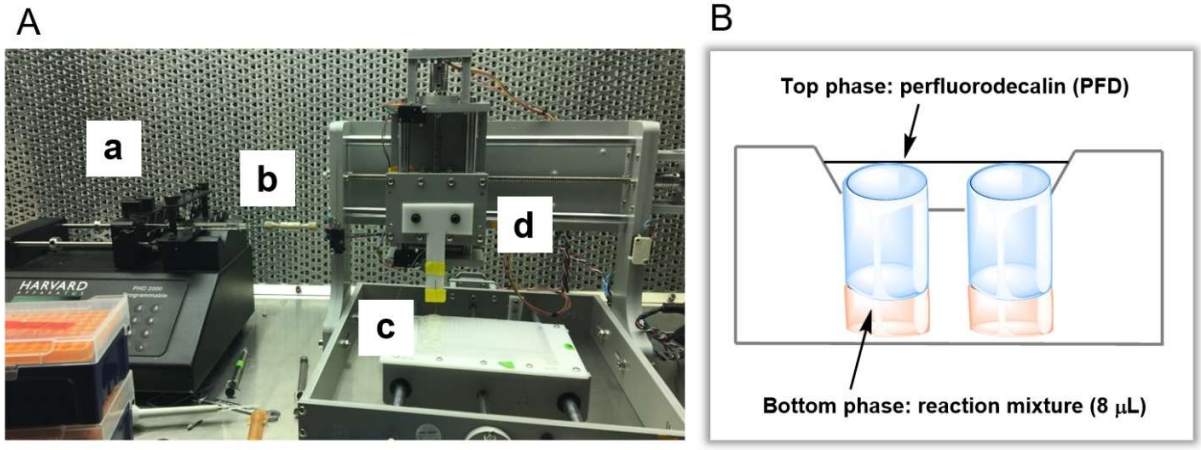

Figure S6. Setup for automated droplet generation. (A) Generation of droplets from 1536 well plates with (a) syringe pump, (b) syringe, (c) 1536 microwell plate, (d) XYZ-position manipulator with well plate stage. (B) Zoomed in depiction of wells containing reaction mixture and PFD.

nESI-MS and ESI-MS Analysis

For nESI-MS analysis, connections from PFA tubing to nanoelectrospray emitters were formed using zero dead-volume Picoclear™ unions (New Objective, Woburn, MA). nESI emitters were pulled from 75 or 100 µm i.d. x 360 µm o.d. fused silica capillary to an i.d. of 30 µm (FS360-50-30-CE, New Objective, Woburn, MA). Electrospray potential of 1.75 kV was applied to the exterior of the platinum coated emitters, with 35 V applied to the sample cone. Mass spectrometry analysis was performed on a Micromass Quattro Ultima triple-quadrupole mass spectrometer (Waters, Milford, MA). Nitrogen cone gas emerging from sampling inlet was set to 125 L/h to help

stabilize the electrospray. For data analysis in MS-only scanning, droplet response was reported as the average of three data points in the center of each droplet. For MS-MS analysis, 5 data points were used. Flow rates to nESI-MS analysis matched droplet generation flow rates, except in experiments testing higher throughputs, which were flowed at 1500 nL/min.

For work using a standard electrospray source, ESI voltage was 3.0 kV, the source was heated to 100 ºC, the cone gas was set at 225 L/h, the desolvation gas was 300 L/h and 200 ºC. The nebulizing gas flow was not measured, but it was adjusted to one half turn of the dial.

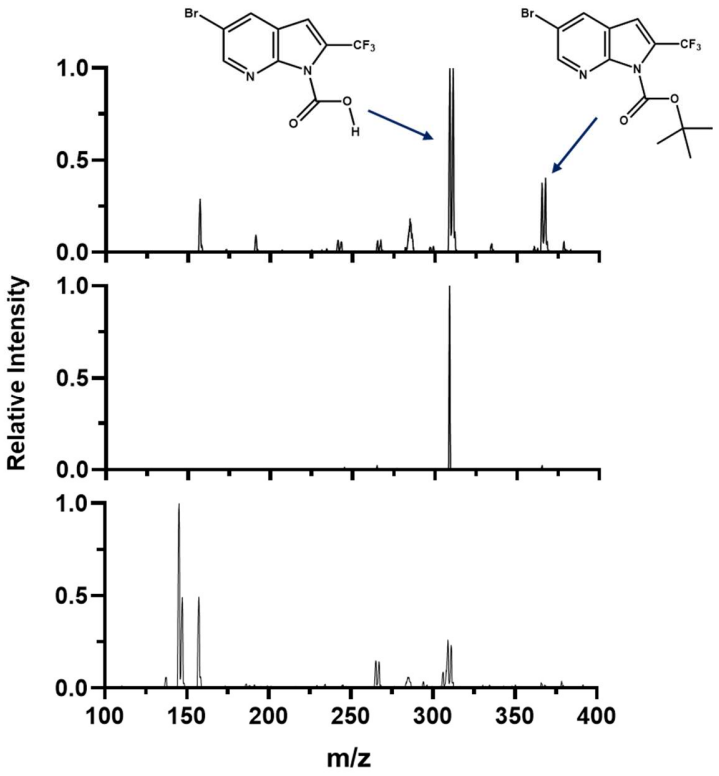

Figure S7. Comparison of ESI and nESI analysis of trifluoromethyl azaindole, with predicted structures for intact molecule (Right) and loss of t-butyl group (Left). Arrows point to m/z peaks associated with each structure. (Top) nESI-MS analysis affording observation of the labile MH^+ molecular ion. While the 309/311 m/z fragments are the most prominent, the 365/367 m/z molecular ions were readily apparent. (Middle) nESI-MS-MS analysis of 365 m/z ion at 10 eV collision energy. Fragmentation of the 365 m/z ion showed almost complete conversion to 309 m/z ion, validating that molecular ions can fragment to form the 309/311 m/z ions observed in MS spectra. (Bottom) ESI-MS analysis of same sample. In this spectrum, molecular ions are no longer observed.

We found that nESI could promote the formation of molecular ions even when ESI could not (**Figure S7**), further highlighting the potential utility of a nESI-MS in screening applications. Samples composed of 50 mM trifluoromethyl azaindole before dilution were examined by both nESI-MS and ESI-MS analysis. nESI-MS analysis of sample containing analyte at a flow rate of 800 nL/min yielded spectra that showed the intact MH^+ molecular ion at m/z=365 and 367, along with prominent fragments at 309 and 311. MS-MS analysis of the 365 m/z ion showed the formation of the m/z=309 ion with very little energy applied, validating it as a fragment of the

original molecular ion. When using the standard ESI source with sample flow at 100 µL/min, the molecular ion was not visible as nearly complete fragmentation was observed. While some fragmentations can be easily predicted (e.g. Boc protection), predicting fragmentation patterns and performing more in-depth structural assignments would not be amenable to HT work, making an ionization method that maximizes the chance of observing molecular ions more favored.

Pfizer Compound Library Screen

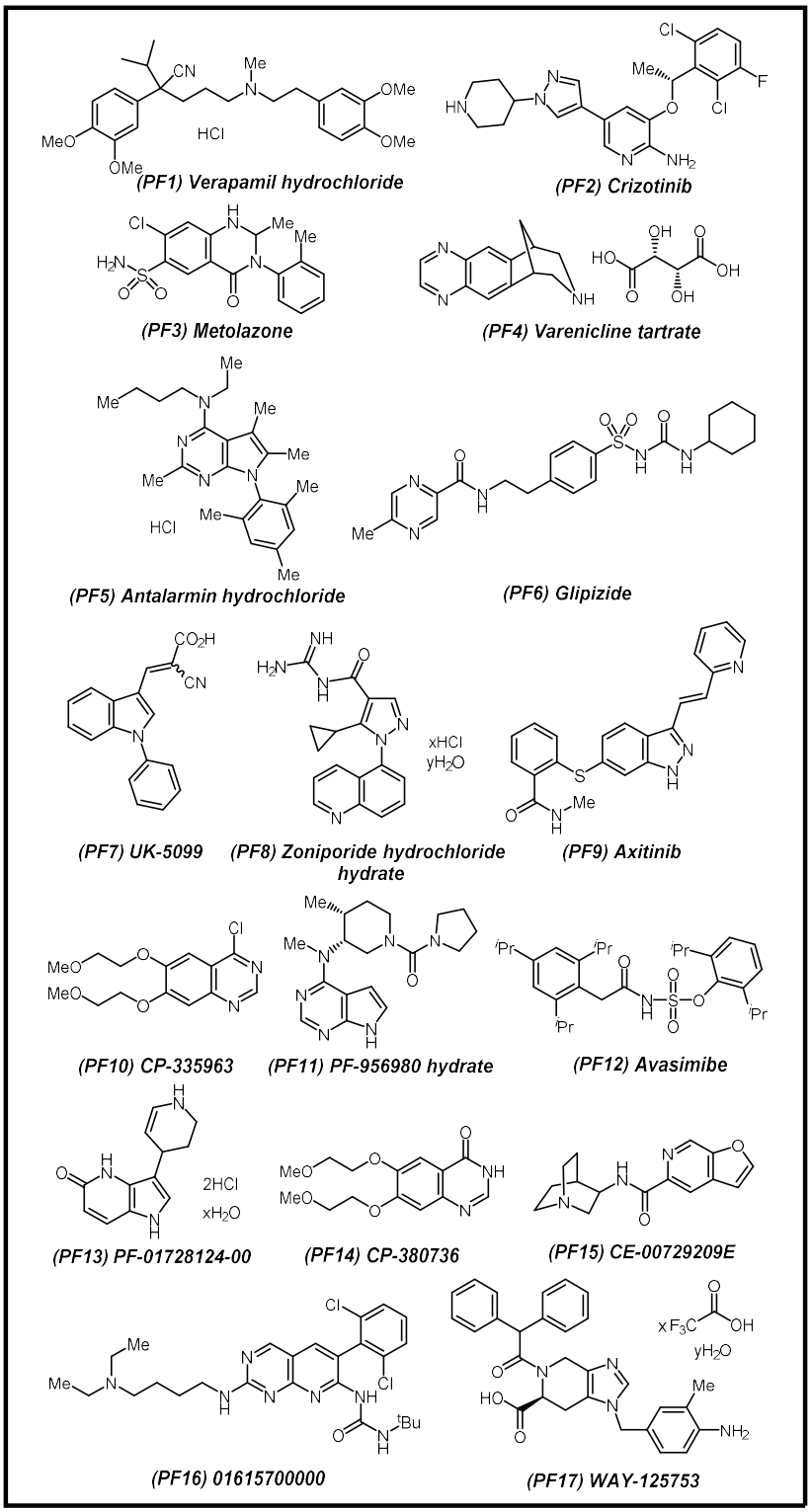

Figure S8. Library of Pfizer compounds investigated in screen.

2 µmol Well Plate Screen of Perfluoroalkylation Reactions

The general procedure described on page S7 was used to prepare the well plate screens performed in Fig. 3 of the main text.

0.1 mmol Scale-up of Perfluoroalkylation Reactions

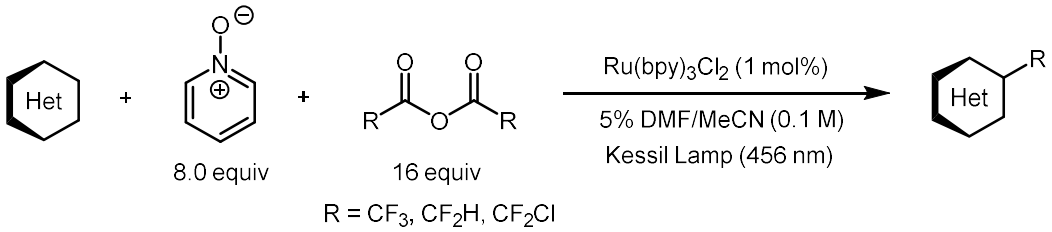

Photocatalyst (1 mol%), pyridine N-oxide (8 equiv), substrate (0.1 mmol), and 5% DMF/acetonitrile (0.2 M) were added to a 1 dram vial charged with a stir bar. The solution was sparged with a stream of nitrogen gas for 5 min. Acetic anhydride (16 equiv) was subsequently added, and the solution was stirred for 10 min to facilitate formation of the acylated species. The reaction was stirred and irradiated for 16 h with a 456 nm Kessil lamp (positioned 5 cm away). A fan was used to keep the reactions at ambient temperatures. Workup was performed by diluting the reaction with dichloromethane and washing with 1 N HCl (x), saturated $NaHCO_3$ (x1), and then brine (x1). The organic layer was dried over sodium sulfate before filtering and concentrating under reduced pressure. The crude product was then purified by column chromatography to afford the desired perfluoroalkylation product(s).

Products Not Isolable Upon Scale-up

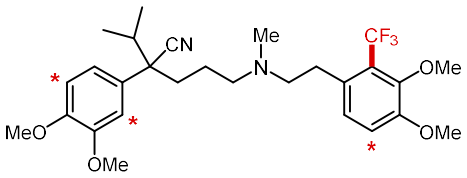

Low yields of product regioisomers prevented successfu isolation

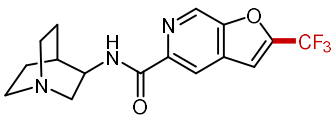

Product decomposition observed upon column chromatography

Product Isolated Upon Scale-up

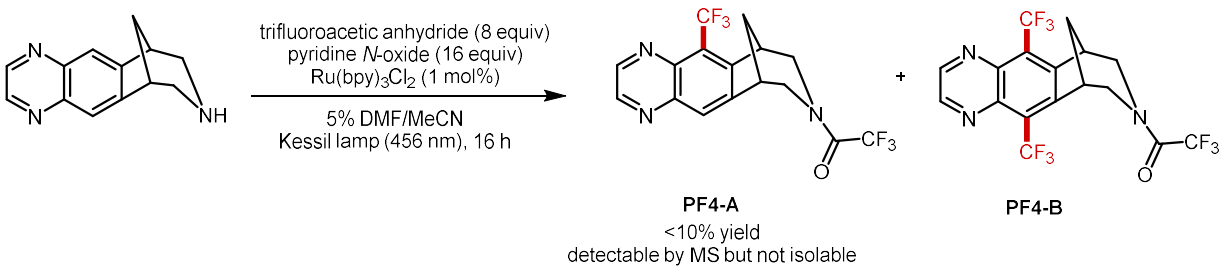

1-((6R,10S)-5,11-bis(trifluoromethyl)-6,7,9,10-tetrahydro-8H-6,10-methanoazepino[4,5g] quinoxalin-8-yl)-2,2,2-trifluoroethan-1-one (PF4-B)

The reaction was run according to the 0.1 mmol scale-up procedure described above and was purified by column chromatography (0% to 15% ethyl acetate in hexanes) to afford the title compound (20 mg, 45%) as a pale yellow solid. R_f = 0.60 (ethyl acetate/hexanes 1:4; UV). ^{1}H NMR (700 MHz, $CDCl_3$) δ 9.01 (d, *J* = 6.3 Hz, 1H), 4.70 – 4.60 (m, 1H), 4.24 (d, *J* = 13.3 Hz, 1H), 4.11 (s, 1H), 4.03 (s, 1H), 3.71 (d, *J* = 13.2 Hz, 1H), 3.32 (d, *J* = 13.4 Hz, 1H), 2.46 (q, *J* = 5.8, 5.2 Hz, 1H), 2.24 (d, *J* = 11.8 Hz, 1H). ^{13}C NMR (176 MHz, $CDCl_3$) δ 157.02 (q, *J* = 35.9 Hz), 146.31 (d, *J* = 110.4 Hz), 144.94 (d, *J* = 14.6 Hz), 140.05 (d, *J* = 30.3 Hz), 123.51 (q, *J* = 215.1 Hz), 116.74 (q, *J* = 286.9 Hz), 50.06, 47.68, 40.39, 39.66 (q, *J* = 3.8 Hz), 39.43 (q, *J* = 3.8 Hz). ^{19}F NMR (377 MHz, $CDCl_3$) δ -55.08, -55.55. HRMS (ESI) m/z $[M + H]^+$ calcd for: $C_{17}H_{10}F_9N_3O$: 444.0753; found: 444.0751. IR (neat): v = 2925, 2853, 1694, 1583, 1561, 1456, 1420, 1394, 1316, 1277.

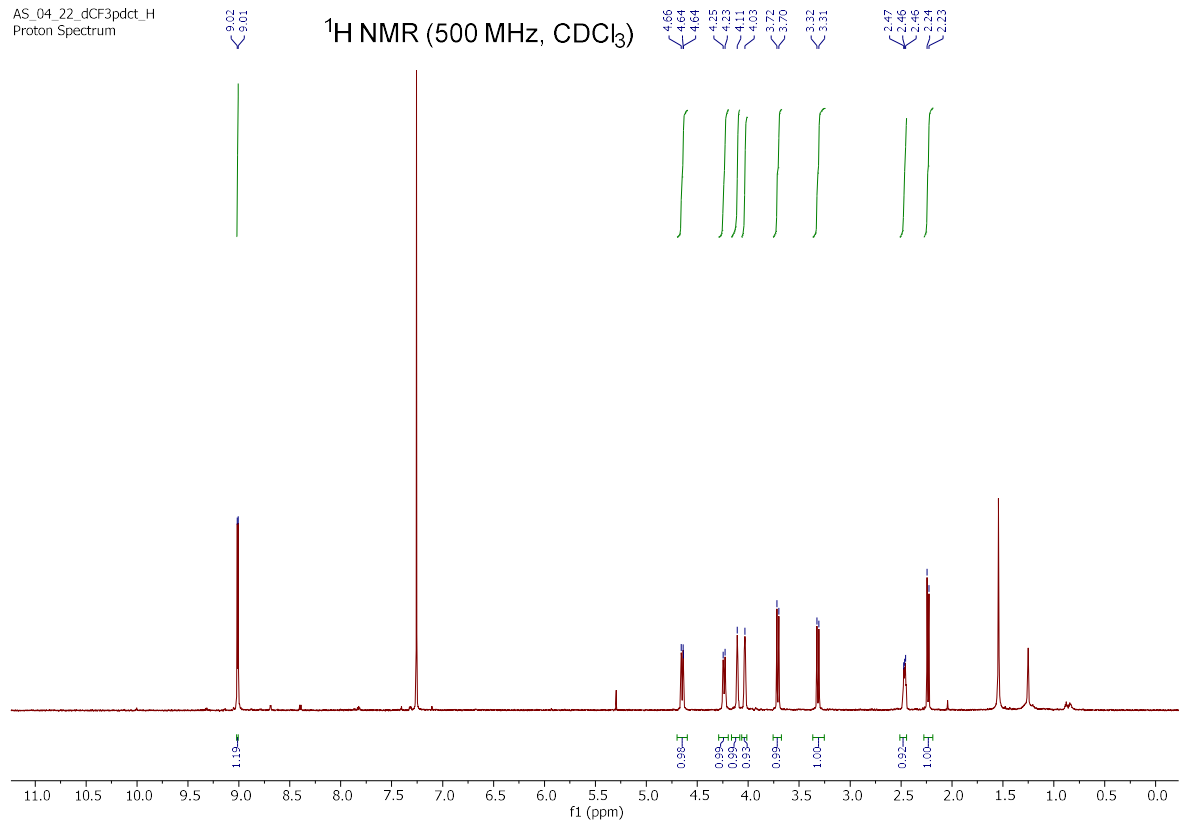
AS_04_22_dCF3pdct_H
Proton Spectrum
^{1}H NMR (500 MHz, $CDCl_3$)
f1 (ppm)

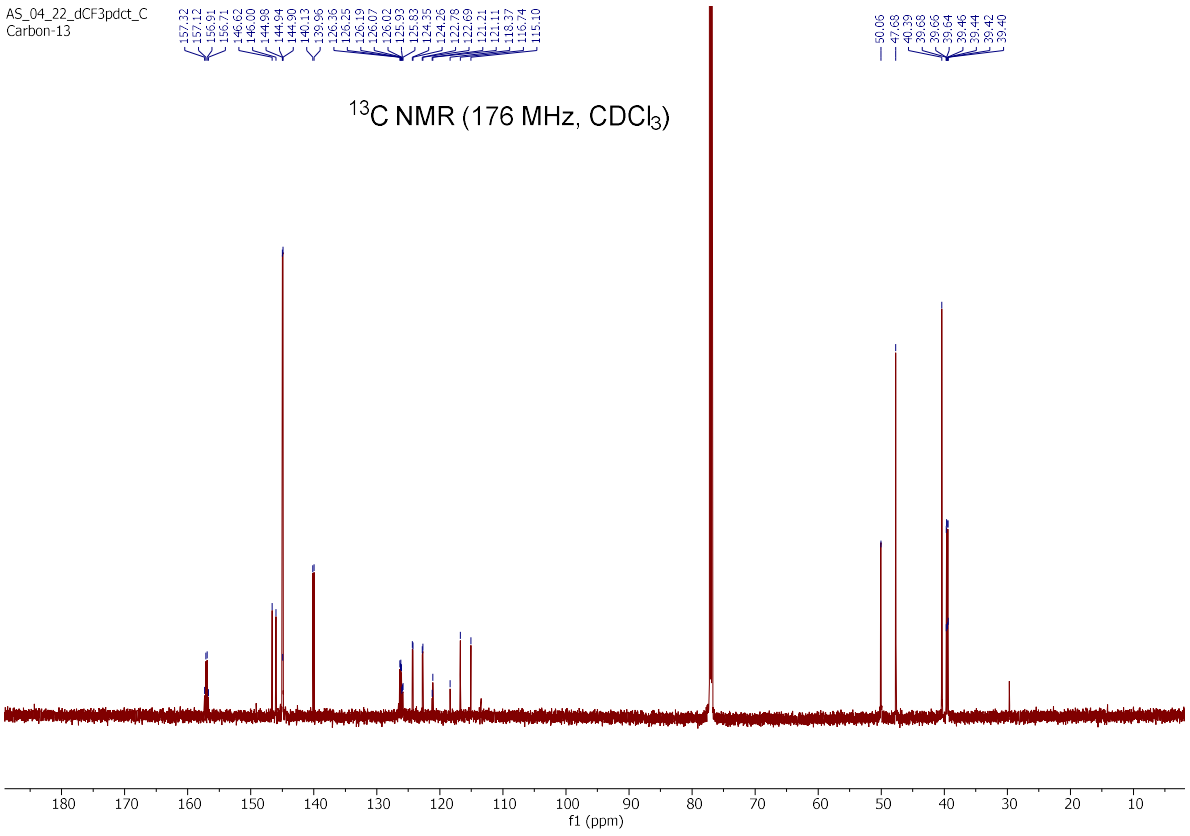
AS_04_22_dCF3pdct_C
Carbon-13
^{13}C NMR (176 MHz, $CDCl_3$)
f1 (ppm)

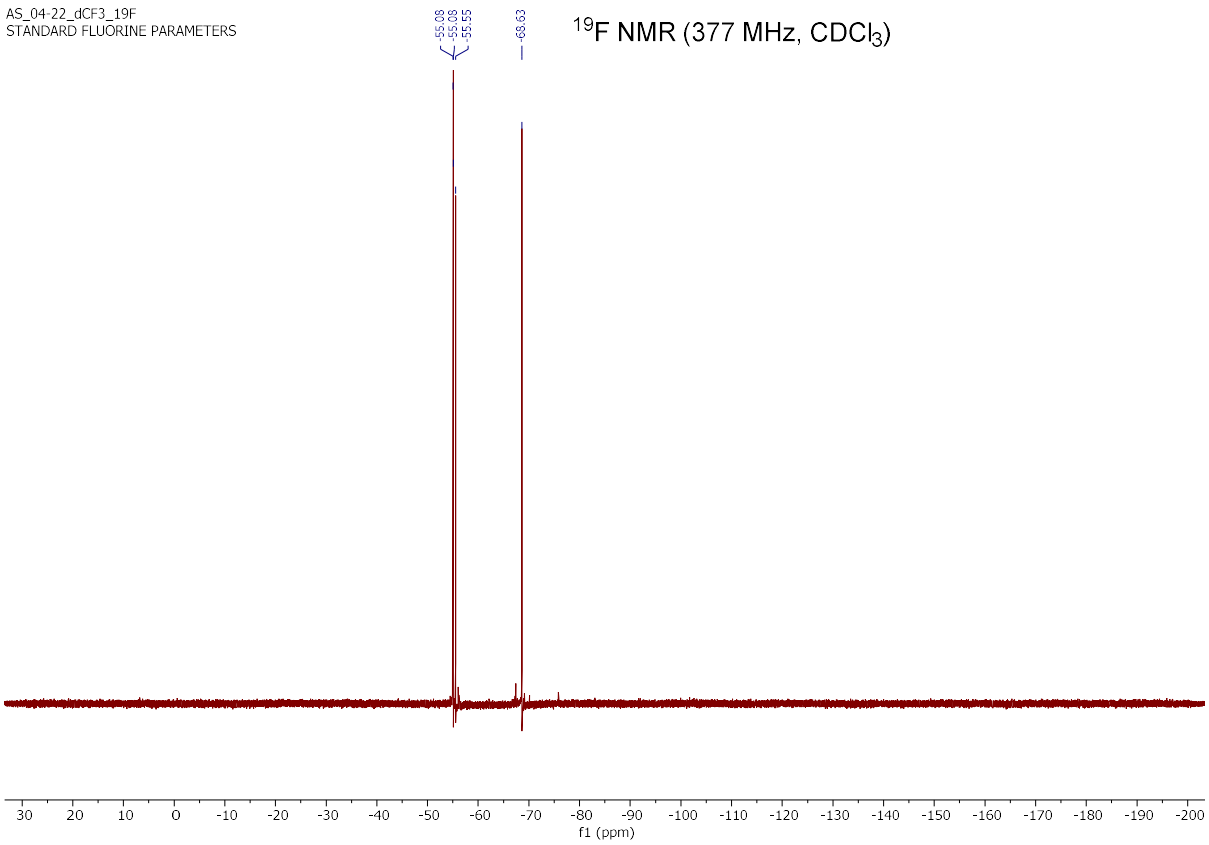

^{19}F NMR (377 MHz, $CDCl_3$)

Caffeine Trifluoromethylation Optimization Screen

3 µmol Well Plate-Based Caffeine Trifluoromethylation Optimization Screen

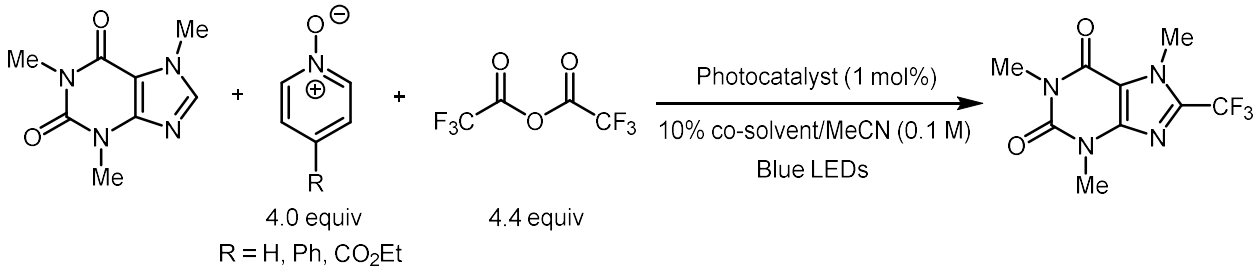

Photocatalyst (1 mol%), pyridine *N*-oxide (4.0 equiv), and 10% co-solvent/acetonitrile (0. M) were added to a vial charged with a stir bar. The solution was sparged with a stream of nitrogen gas for 5 min. Trifluoroacetic anhydride (4.4 equiv) was subsequently added, and the solution was stirred for 10 min to facilitate formation of the acylated species. Separate solutions of caffeine (3 µmol) in 10% co-solvent/acetonitrile (0.2 M) were also prepared. 10 µL of each solution were combined in a 384 well plate to form the final reaction solution. Reactions were irradiated using the photoreactor setup described above without mixing.

As shown in Figure 4A and B in the main text, the following photocatalysts and co-solvents were screened:

Photocatalysts: (A) $Ru(bpy)_3Cl_2$, (B) $[Ir(ppy)_2(dtbbpy)]PF_6$, (C) $[Ir(dF(CF_3)ppy)(dtbbpy)]PF_6$, (D) $Ir(ppy)_3$

Co-solvents: (1) MeCN, (2) $MeNO_2$, (3) CH_2Cl_2, (4) DMF, (5) DMA, (6) DMSO

0.3 mmol Scale-up of Caffeine Trifluoromethylation Screen Reactions

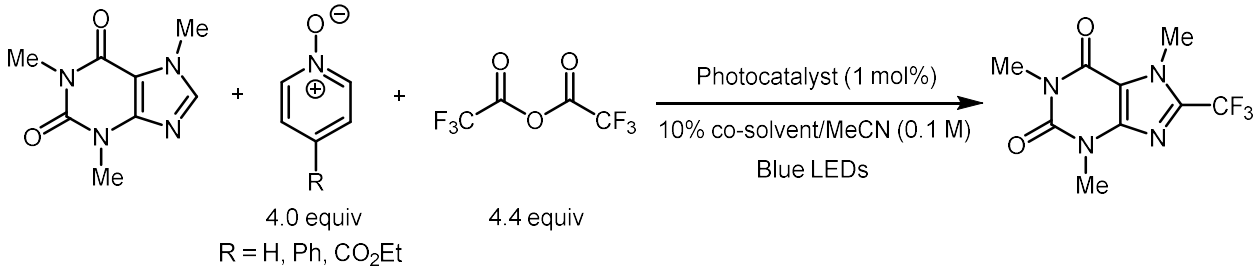

Photocatalyst (1 mol%), pyridine *N*-oxide (4.0 equiv), and 10% co-solvent/acetonitrile (0.1M) were added to a vial charged with a stir bar. The solution was sparged with a stream of nitrogen gas for 5 min. Trifluoroacetic anhydride (4.4 equiv) was subsequently added, and the solution was stirred for 10 min to facilitate formation of the acylated species. Separate solutions of caffeine (3 mmol) in 10% co-solvent/acetonitrile (0.2 M) were also prepared. 10 µL of each solution were combined in a 96 well plate to form the final reaction solution. Reactions were irradiated using the photoreactor setup described above without mixing.

As shown in Figure 4C in the main text, the following five photocatalyst, *N*-oxide, and co-solvent combinations were screened:

Sample number 1: 10% DMA, $[Ir(ppy)_2(dtbbpy)]PF_6$ + 4-phenylpyridine N-oxide
Sample number 2: 10% DMF $[Ir(dF(CF_3)ppy)_2(dtbbpy)]PF_6$ + pyridine N-oxide
Sample number 3: 10% DCM $[Ir(ppy)_2(dtbbpy)]PF_6$ + 4-CO_2Et pyridine N-oxide
Sample number 4: 10% DMF $[Ir(ppy)_2(dtbbpy)]PF_6$ + 4-phenylpyridine N-oxide
Sample number 5: 10% DMF $Ir(ppy)_3$ + 4-CO_2Et pyridine N-oxide

nESI-MS Traces for 72 Reaction Condition Screen

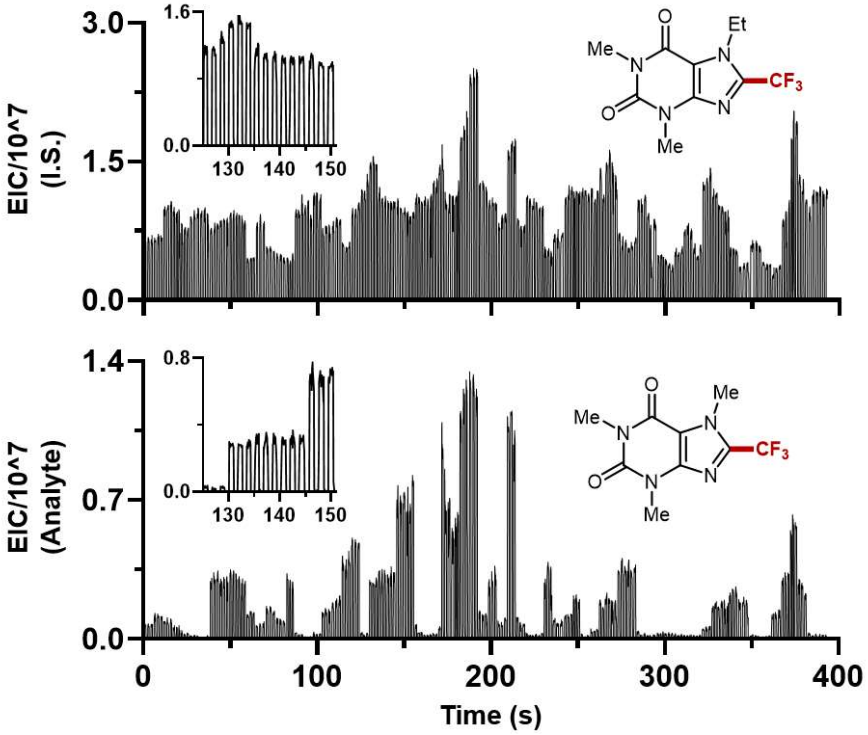

Figure S9. Internal standard trace (m/z = 277→192, top) and product MS-MS trace (m/z = 263→206, bottom) across 72-reaction screen. Insets are enlarged regions for 125-150s (left) and molecular structures (right).

Addressing Variable Analyte Ionization Efficiency

Formation of gas phase analyte ions necessary for MS detection can be greatly affected by the composition of the sample matrix (Figure S10). In order to allow for direct comparison of product formation across samples where reaction parameters are varied, the effects of sample matrix on analyte ionization need to be accounted for.

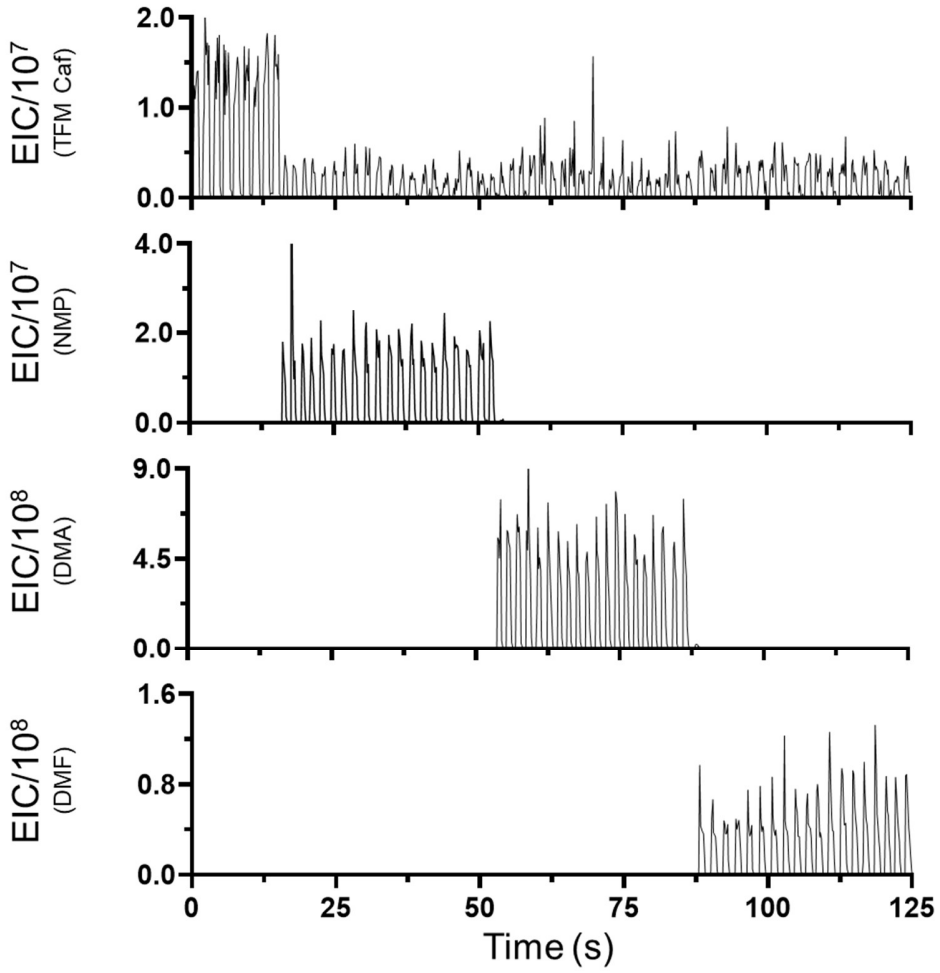

Figure S10. Effect of co-solvent on detection of trifluoromethylated caffeine analyte. 50 mM analyte was dissolved in either acetonitrile or acetonitrile with 10% cosolvent, followed by a 500:1 dilution with 50:50 methanol:water, 1% formic acid. (Top) MS trace (m/z=263) for analyte. Droplets within the first 13 seconds were composed of trifluoromethylated caffeine dissolved in acetonitrile. Proceeding droplets had 10% of one of three cosolvents (NMP, DMA, or DMF). Each caused a massive decrease in response, possibly owing to competition for surface ionization during the electrospray process (2nd, 3rd, and 4th traces). In descending order, MS traces for NMP (m/z=100), DMA (m/z=88) and DMF (m/z=74).

To address variable matrix effects on analyte ionization, three separate approaches were explored. The first method was the use of standard addition, which is a commonly employed tactic for addressing samples that have unknown matrix effects. For this approach, each sample of interest was further split into two samples to analyze. The first was made using a 500:1 dilution as described in Figure S10. The second used the same dilution factor, but the solvent contained 15 μM trifluoromethylated caffeine standard. Because both samples contain the same matrices and therefore similar analyte ionization efficiencies, taking the ratio of the two responses gives a measure of analyte concentration that accounts for matrix effects. The second method utilized a higher dilution factor (10,000x vs. 500x) before droplet generation. By increasing the dilution and therefore further reducing the concentration of matrix components, we sought to reduce matrix effects to a negligible level. Finally, the addition of an internal standard was examined. For our caffeine trifluoromethylation reaction, we chose to use trifluoromethylated ethyl theophylline as the internal standard, as it only varies in structure by a single methylene group. This change is easily discernable by MS but should not significantly affect ionization. Trifluoromethylated ethyl theophylline was present in the dilution phase at a concentration of 30 μM. For each droplet sample, the response for analyte could be normalized against internal standard, which should show similar changes in ionization from variable matrices. Each method has associated pros and cons, which are shown in Table S1.

	Standard Addition (Std. Add.)	**High Dilution**	**Internal Standard (IS)**
Summary	Two fractions from each sample were taken. One was diluted with blank diluent, the other diluted with product standard. A ratio of the MS responses was reported (I_x/I_{x+s}).	Dilution factor was increased from 500x to 10,000x in order to minimize matrix effects.	A structural homologue of the analyte was added to the diluent. Both m/z for analyte and for IS are monitored. Each droplet response was listed as a ratio (A/IS).
Pros	• Directly accounts for matrix effects	• Simple to implement • Does not require any molecular standards	• Directly accounts for matrix effects and some sample handling errors • Shows the highest precision in droplet analysis
Cons	• Halves throughput • Found to have lowest precision and most affected by sample matrix of the 3 methods.	• Analyte is diluted also, which can hurt detection limits • Will not account for any remaining matrix effects	• Generation of new IS may be required when examining a new reaction

Table S1. Comparison of examined methods for addressing matrix effects.

Each method was examined for its utility as a quantitative tool. First, the capability of each method to account for matrix effects was examined. This was performed by dissolving trifluoromethylated caffeine (50 mM) in acetonitrile containing 0, 4, or 10% DMF. A successful method would be capable of giving a uniform response even with DMF present. The overall results are shown in Figure S11, with representative droplet traces for each shown in Figures S12-14. All three methods yielded significantly improved results relative to a control run in which no additional measures were taken.

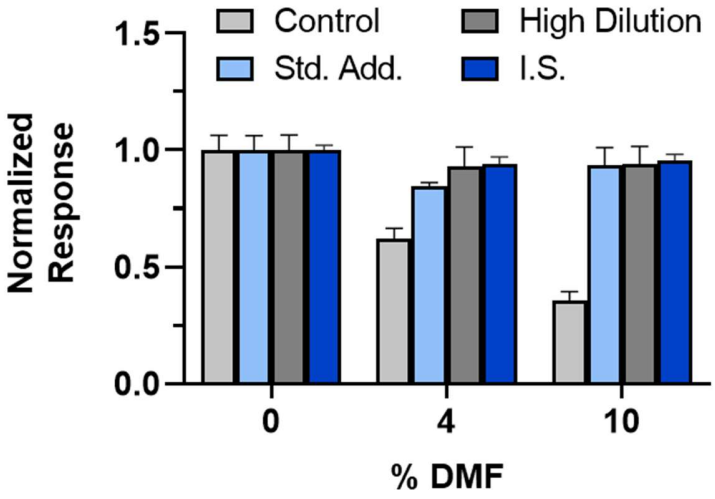

Figure S11. Comparison of performance across high dilution, standard addition (Std. Add.) and internal standard (I.S.) methods for addressing variable trifluoromethylated caffeine ionization in droplet nESI-MS-MS analysis. Each bar represents the results from 15 separate samples analyzed in triplicate. Control samples consisted of trifluoromethylated caffeine response from original conditions with no extra measures employed. Responses are normalized within each method.

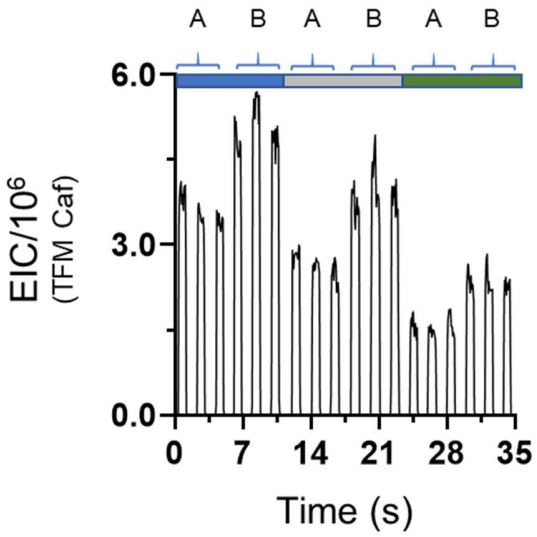

Figure S12. Trifluoromethylated caffeine MS-MS trace (m/z = 263→206) for standard addition method. Droplets with "A" designation were diluted normally, while "B" designation denotes droplets that were diluted with product standard solution. 0% DMF (blue bar), 4% DMF (grey bar), and 10% DMF (green bar) showed variable ionization, but by normalizing A samples against B samples (A/B), these changes can be accounted for.

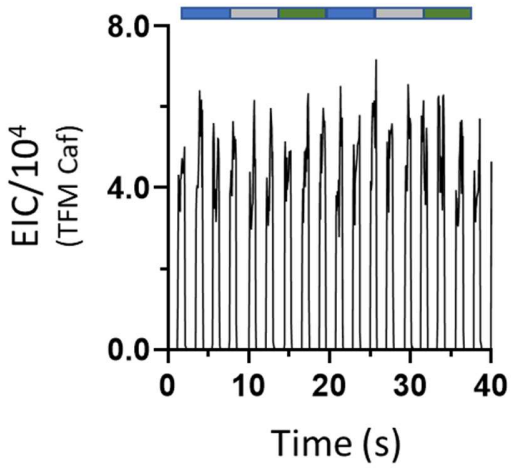

Figure S13. Trifluoromethylated caffeine MS-MS trace (m/z = 263→206) obtained from high dilution method. 0% DMF (blue bar), 4% DMF (grey bar), and 10% DMF (green bar) showed no notable differences in ionization efficiency.

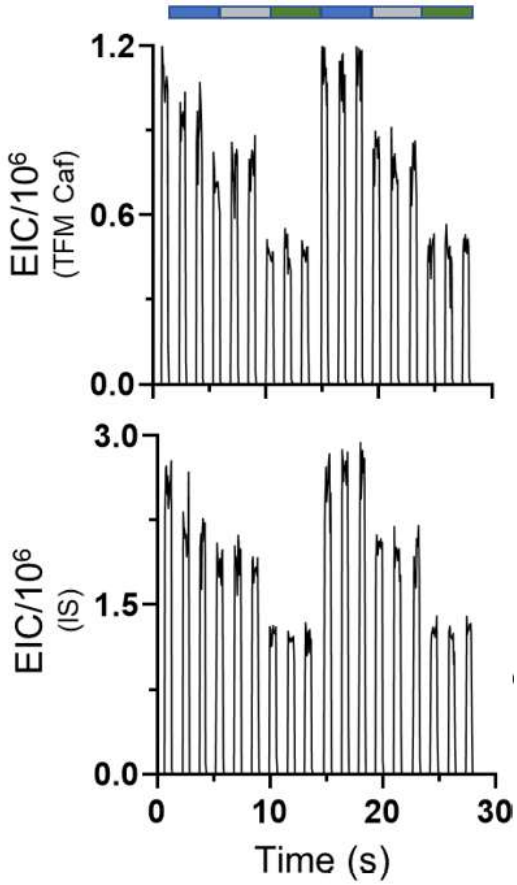

Figure S14. Trifluoromethlated caffeine MS-MS trace (m/z = 263→206, top) and trifluoromethylated ethyl theophylline (m/z = 277→192, bottom) for internal standard method. 0% DMF (blue bar), 4% DMF (grey bar), and 10% DMF (green bar) showed variable ionization, but by normalizing each droplet's analyte response against its internal standard response (A/IS), these effects can be accounted.

To show how each method may perform in a screening environment, a small mock screen was created that represented different yields for the trifluoromethylation reaction, as well a major changes in solvent, upwards of 50% of one of three cosolvents (Table S2). Results are shown in Figure S15. The use of an IS showed the lowest RSD across all sample concentrations. This points to it as the best choice for monitoring smaller changes in product formation, though all three methods were found to be generally capable of detecting the changes in product concentration.

	A	B	C	D	E	F	G
Simulated Yield (% conversion)	5	5	5	15	10	5	5
	10	10	10	20	15	10	10
	15	15	20	25	20	15	20
	20	25	25	30	30	20	30

Table S2. Array of samples created for data in Figure SG. Solvent systems are labelled in column headers and are as follows: (A) 100% MeCN, (B) 10% CH_2Cl_2, (C) 10% NO_2Me, (D) 10% DMF, (E) 50% CH_2Cl_2, (F) 50% NO_2Me, (G) 50% DMF.

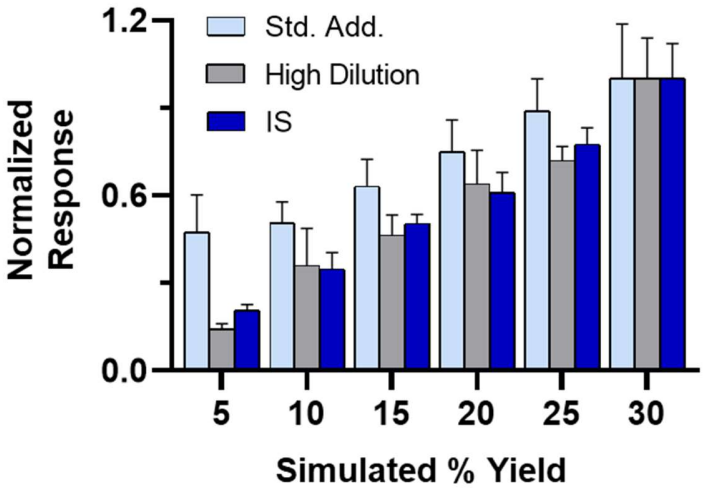

Figure S15. Compiled results from mock screen. The responses for all samples at any given % yield were averaged before plotting. All three methods showed the expected behavior (average response increased with increasing concentration) across all concentrations, showing the potential of each to evaluate samples in a screening capacity.

Novartis Compound Screen

Novartis Library Compounds Screened

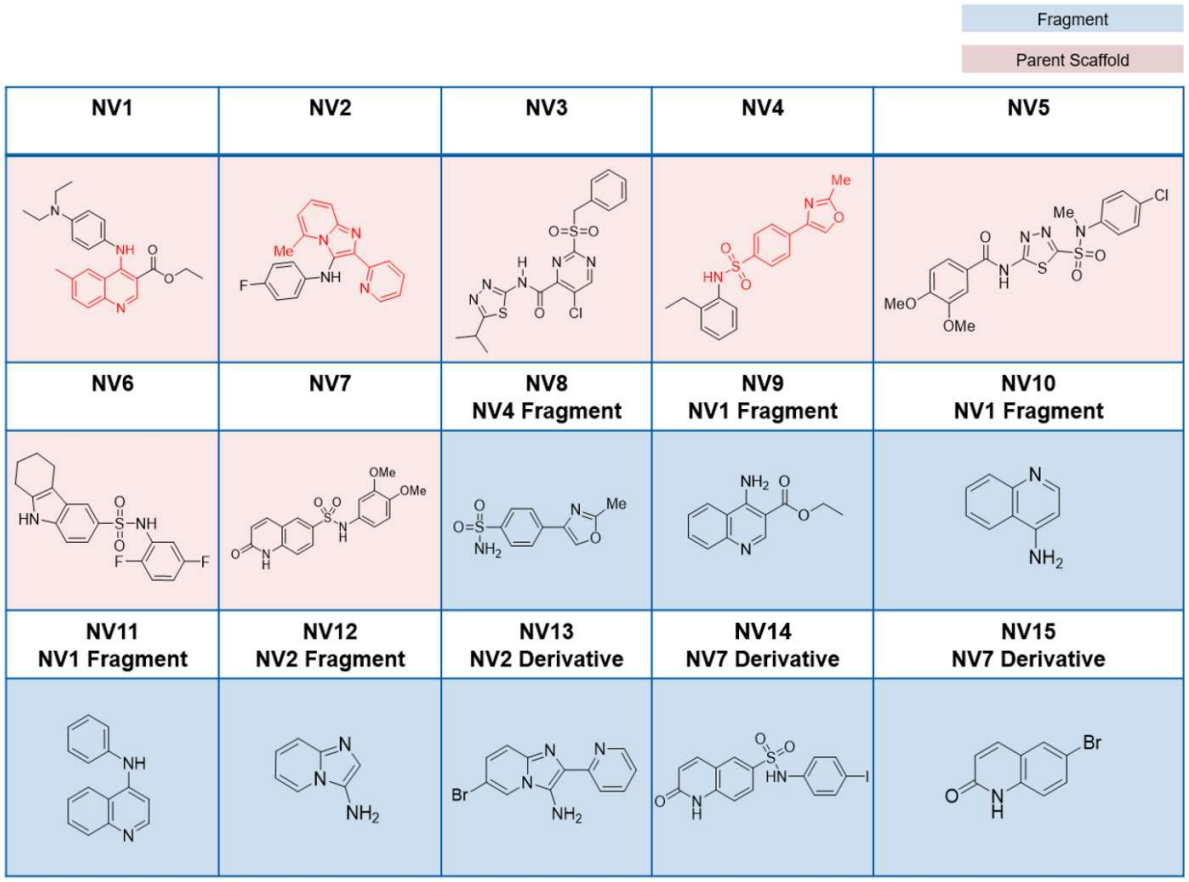

Figure S16. Library of Novartis compounds investigated in screen.

2 µmol Well Plate Screen of Perfluoroalkylation Reactions

The general procedure described on page S7 was used to prepare the well plate screens performed in Fig. 5 of the main text.

0.1 mmol Scale-up of Perfluoroalkylation Reactions

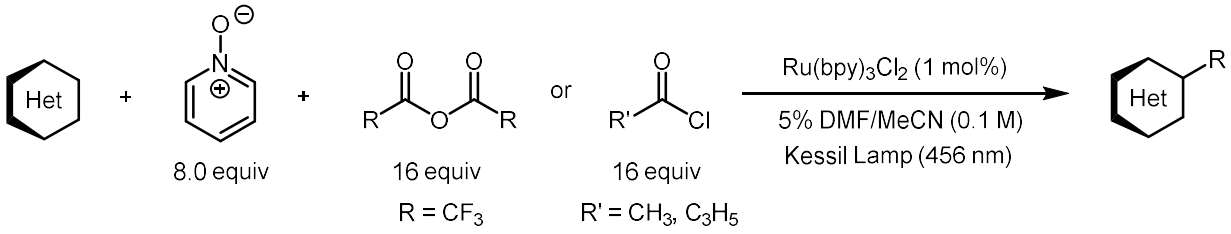

Photocatalyst (1 mol%), pyridine N-oxide (8 equiv), substrate (0.1 mmol), and 5% DMF/acetonitrile (0.2 M) were added to a 1-dram vial charged with a stir bar. The solution was

sparged with a stream of nitrogen gas for 5 min. Acetic anhydride or acid chloride (16 equiv) was subsequently added, and the solution was stirred for 10 min to facilitate formation of the acylated species. The reaction was stirred and irradiated for 16 h with a 456 nm Kessil lamp (positioned 5 cm away). A fan was used to keep the reactions at ambient temperatures. Workup was performed by diluting the reaction with dichloromethane and washing with 1 N HCl (x), saturated $NaHCO_3$ (x1), and then brine (x1). The organic layer was dried over sodium sulfate before filtering and concentrating under reduced pressure. The crude product was then purified by automated mass-directed liquid chromatography to afford the desired perfluoroalkylation product(s).

Compound Characterization Data

Experimental Procedure for Microscale Profiling Assays

Compounds were run through Novartis's standard microscale profiling assays for clearance, permeability, and solubility. These assays were carried out using a Thermo Inspire automation platform with the following components: Thermo Spinnaker microplate robot, LEAP Certus liquid dispenser, Analytik-Jena CyBio Felix liquid handler, Thermo Cytomat incubator, Agilent BioTek EL406 washer dispenser, PerkinElmer Envision plate reader, Agilent BioTek Multiflow dispenser, Agilent PlateLoc sealer, Q Instruments Bioshake shakers, Agilent VSpin centrifuges, and Brooks XPeel plate seal remover.

The microscale clearance assay measures the metabolic stability of a compound - how quickly it is cleared in a solution of human or rat microsomes. It is similar to the assay described in Fonsi et al., 2008[65]. The CLint values generated measure the half-life of the compound divided by the protein concentration in the assay. Our binning scheme sets low clearance as <100, medium clearance between 100 and 300, and high clearance >300.

The microscale permeability assay is adapted from the assay described in Di et al., 2011[66]. It uses low efflux cells grown in plates, with an apical well above the cell layer and a basal well below the cell layer. Compounds are put in the apical wells and incubated for two hours, during which some pass through the cell layer into the basal wells. The data output is P apparent (Papp), which measures the ratio of compound in the apical layer to compound in the basal layer.

The microscale solubility assay measures the equilibrium concentration of a compound in aqueous buffer at pH 6.8 (di-sodium hydrogen phosphate/potassium dihydrogen phosphate). Compounds are dissolved in solution and shaken for 17 hours, after which the undissolved solid is pelleted at the bottom of the well and the concentration of dissolved compound is measured by mass spectrometry using a calibration curve.

In addition to the profiling assays, these compounds were run through the RLUC assay to measure inhibition of the renilla luciferase enzyme. It is adapted from the assay described in Ho et al., 2004[67]. The data output is the RLUC AC50, the concentration of compound at which 50% of the renilla luciferase enzyme is inhibited.

(65) Fonsi, M.; Orsale, M.V.; Monteagudo, E. High Throughput Microsomal Stability Assay for Screening New Chemical Entities in Drug Discovery. *Journal of Biomolecular Screening* **2008**, 13 (9), 862-869. (**66)** Di, L., Whitney-Pickett, C., Umland, J. P., Zhang, H., Zhang, X., Gebhard, D. F., Lai, Y., Federico, J. J., 3rd, Davidson, R. E., Smith, R., Reyner, E. L., Lee, C., Feng, B., Rotter, C., Varma, M. V., Kempshall, S., Fenner, K., El-Kattan, A. F., Liston, T. E., & Troutman, M. D. (2011). Development of a new permeability assay using low-efflux MDCKII cells. *Journal of pharmaceutical sciences* **2011**, *100*(11), 4974–4985. **(67)** Ho, P.; Yue, K.; Pandey, P.; Breault, L.; Harbinski, F.; McBride, A. J.; Webb, B.; Narahari, J.; Karassina, N.; Wood, K. V.; Hill, A.; Auld, D. S. Reporter Enzyme Inhibitor Study To Aid Assembly of Orthogonal Reporter Gene Assays. *ACS Chemical Biology* **2013**, *8* (5), 1009–1017.

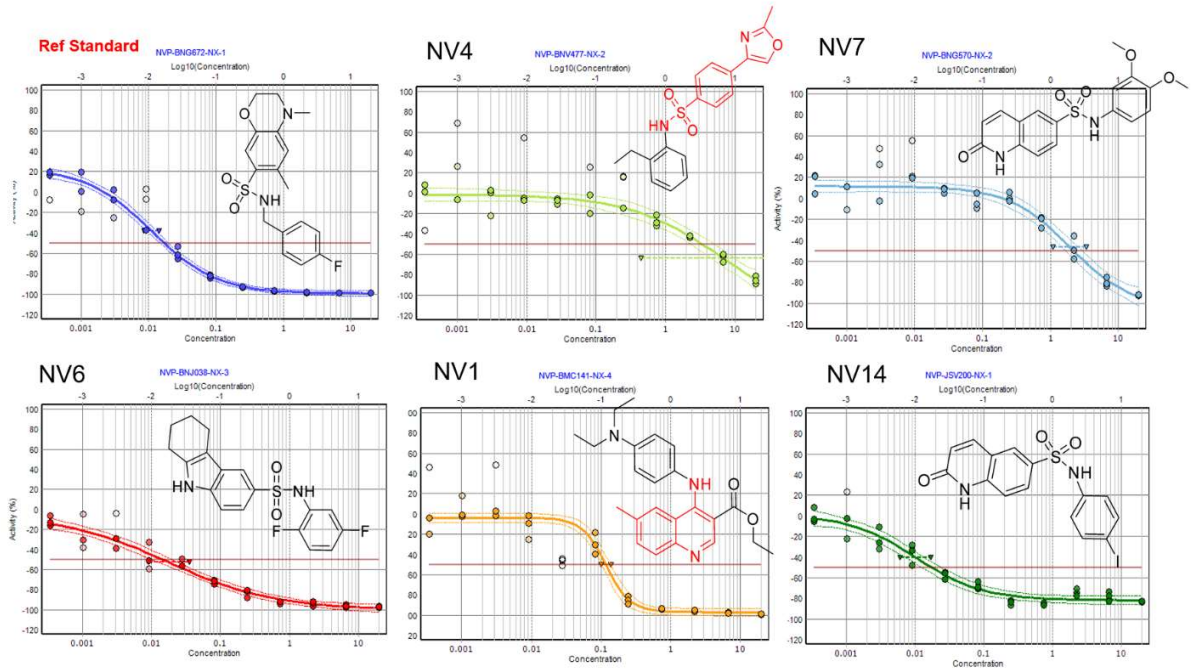

Figure S17. Representative data from RLuc assay studies to determine RLuc AC50 by measuring activity (%) across various compound concentrations.

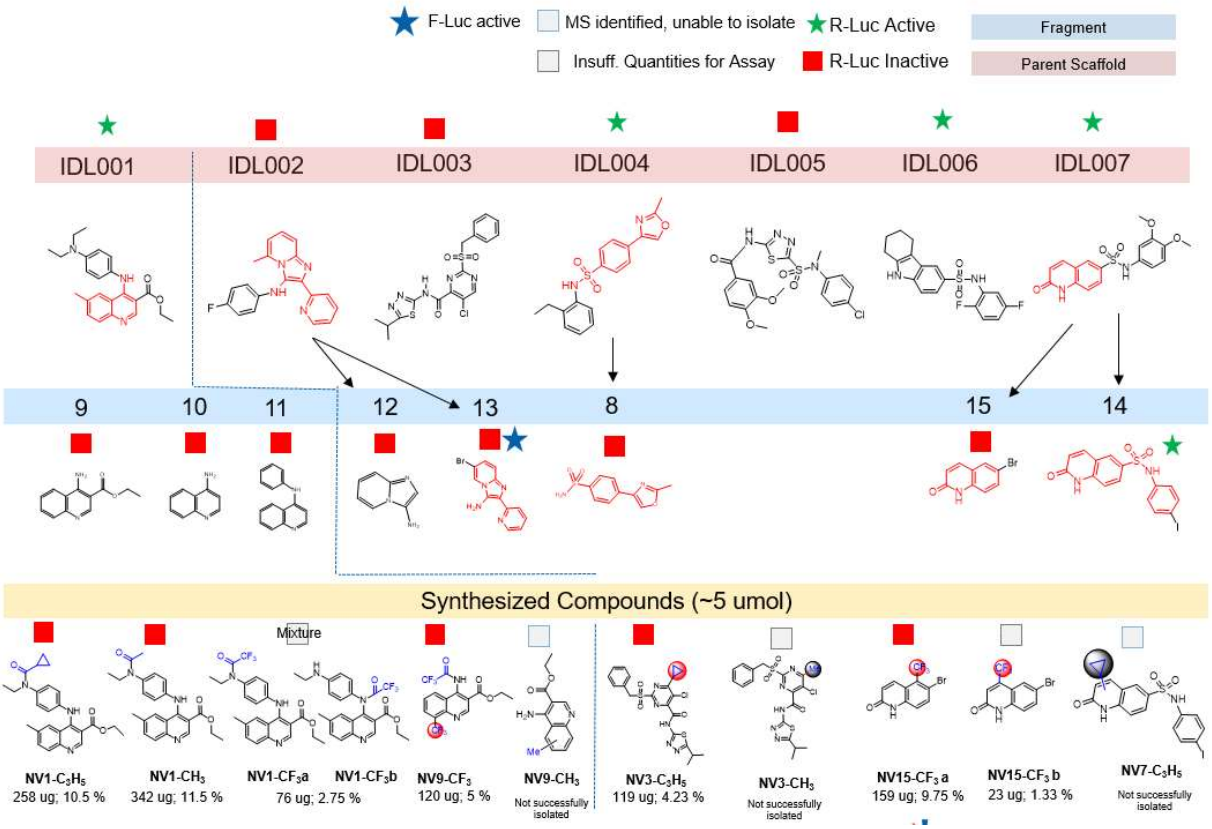

Figure S18. RLuc activity of Novartis library analogues and SAR comparison with parent scaffolds and original fragments.

Compound	RLuc AC50	CLint Human	CLint Rat	MDCK Papp A to B	Solubility (mM at pH 6.8)
NV1	0.116	>700	>700		
NV2	>20	152.8			
NV3	>20	47.8	149.5		
NV4	3.343	136.9			
NV5	>20		112.3	5.895	0.0147
NV6	0.0145			2.703	0.01372
NV7	2.189	52.6	25.9		
NV8	>20				
NV9	>20	285.4	140.8		
NV10	>20				
NV11	>20	124.6	365.6		
NV12	>20				
NV13	>20				
NV14	0.0173			11.552	<0.004
NV15	>20				
NV1-C_3H_5	>20	>700	782.3	0.062	0.00449
NV1-CH_3	>20	>700	446.5	11.605	0.13246
NV3-C_3H_5	>20	40.3	167.2		
NV9-CF_3	>20	165.5	79.9		
NV15-CF_3	>20	<25	<25	21.529	0.04097

Table S3. Microscale profiling assay data for Novartis library analogues and parent scaffolds.

(NV1-parent)

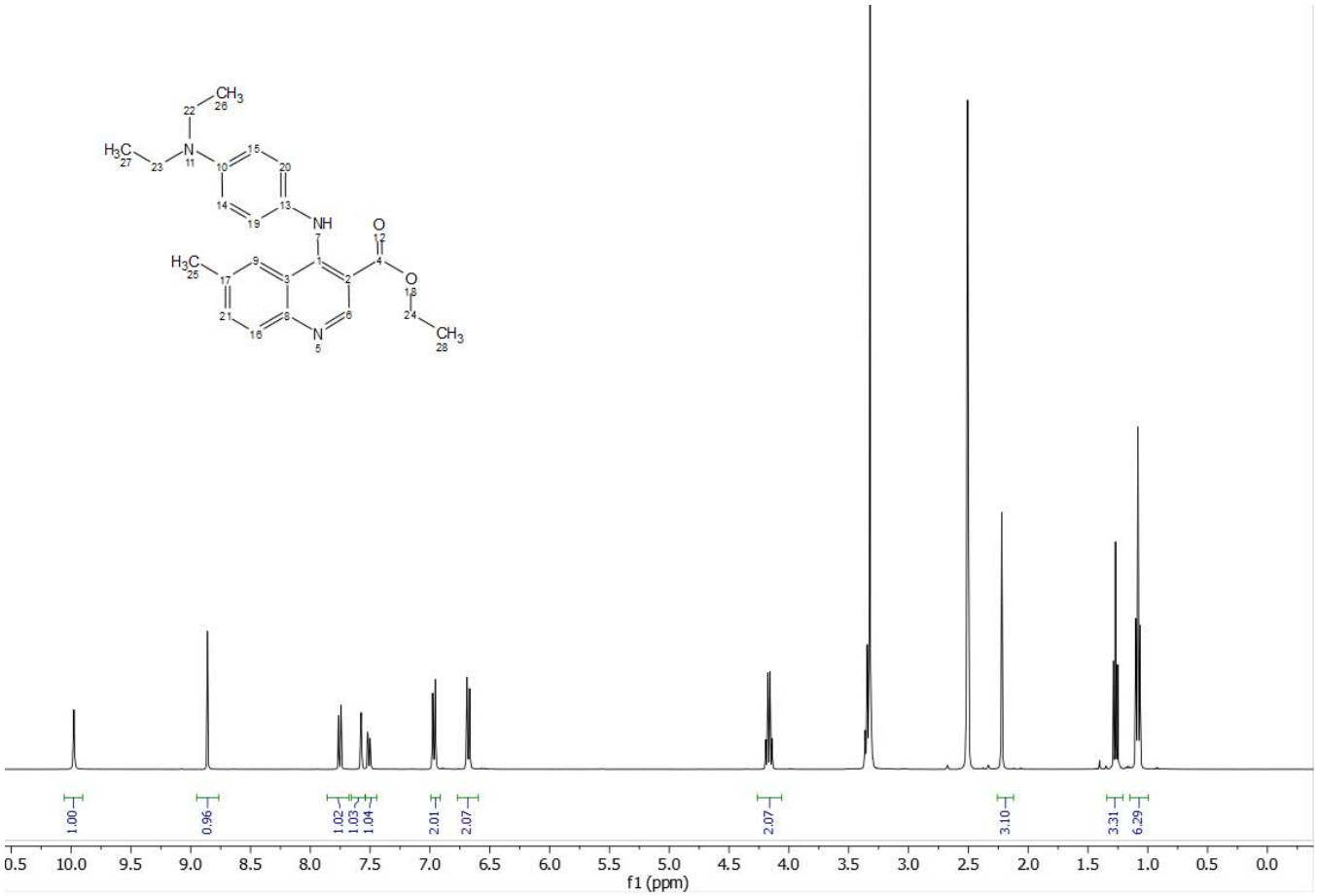

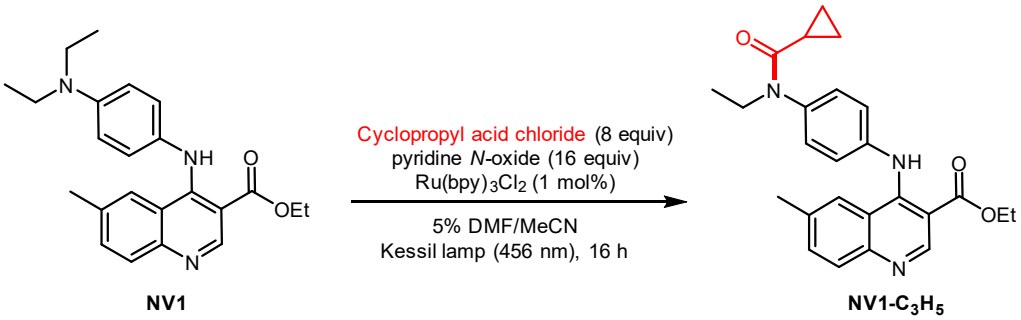

Ethyl 4-((4-(diethylamino)phenyl)amino)-6-methyl-2-(cyclopropyl)quinoline-3-carboxylate (NV1-C_3H_5)

The reaction was run according to the 0.1 mmol scale-up procedure described above and was purified by mass-directed high performance liquid chromatography to afford the title compound (285 ug, 11%). ^{1}H NMR (600 MHz, DMSO) δ 8.89 (s, 1H), 7.91 (s, 1H), 7.88 (d, J = 8.5 Hz, 1H), 7.65 (d, J = 8.5 Hz, 1H), 7.25 (d, J = 8.1 Hz, 2H), 7.14 (d, J = 8.2 Hz, 2H), 3.99 (q, J = 7.2 Hz, 2H), 3.65 (q, J = 7.4 Hz, 2H), 2.38 (s, 3H), 1.14 (t, J = 7.1 Hz, 3H), 1.00 (t, J = 7.2 Hz, 3H), 0.82 – 0.75 (m, 2H), 0.64 – 0.54 (m, 2H). Waters SQ2 single-quad MS: m/z+ 418.4

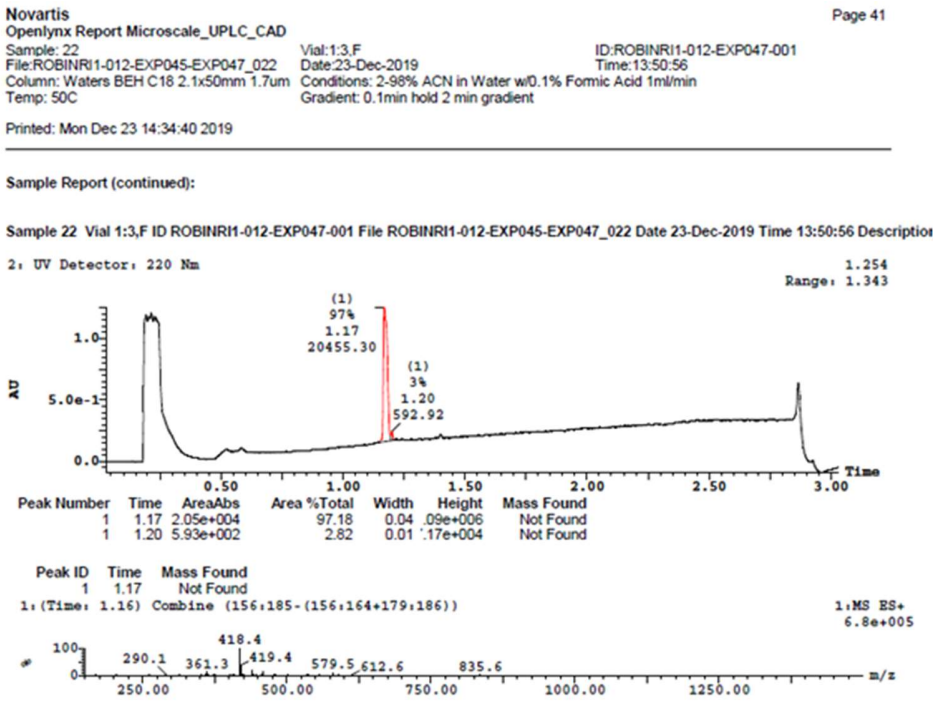

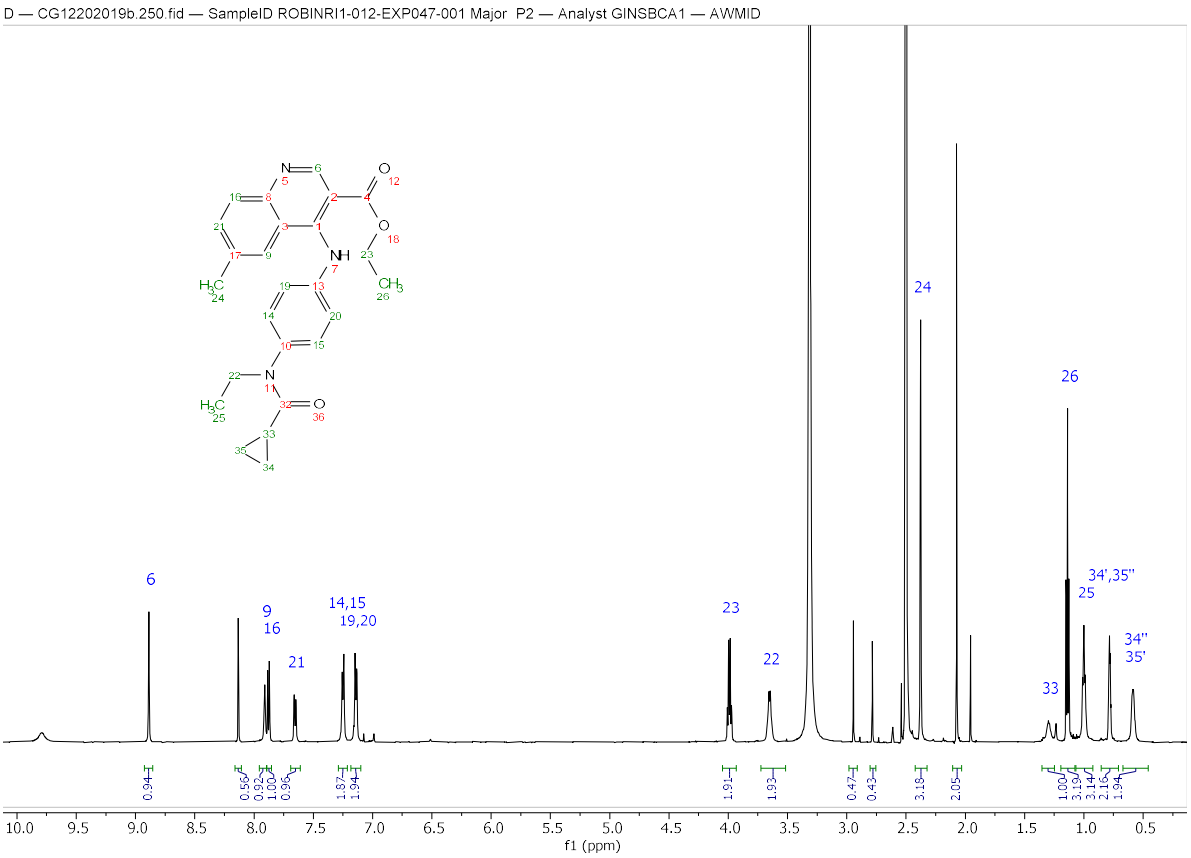
D — CG12202019b.250.fid — SampleID ROBINRI1-012-EXP047-001 Major P2 — Analyst GINSBCA1 — AWMID
6
9
16
21
14,15
19,20
23
22
24
26
33
25
34',35''
34''
35'
0.94
0.56
0.92
1.00
0.96
1.87
1.94
1.91
1.93
0.47
0.43
3.18
2.05
1.00
3.19
3.14
2.15
1.94
10.0 9.5 9.0 8.5 8.0 7.5 7.0 6.5 6.0 5.5 5.0 4.5 4.0 3.5 3.0 2.5 2.0 1.5 1.0 0.5
f1 (ppm)

Predicted 1H-NMR Spectra

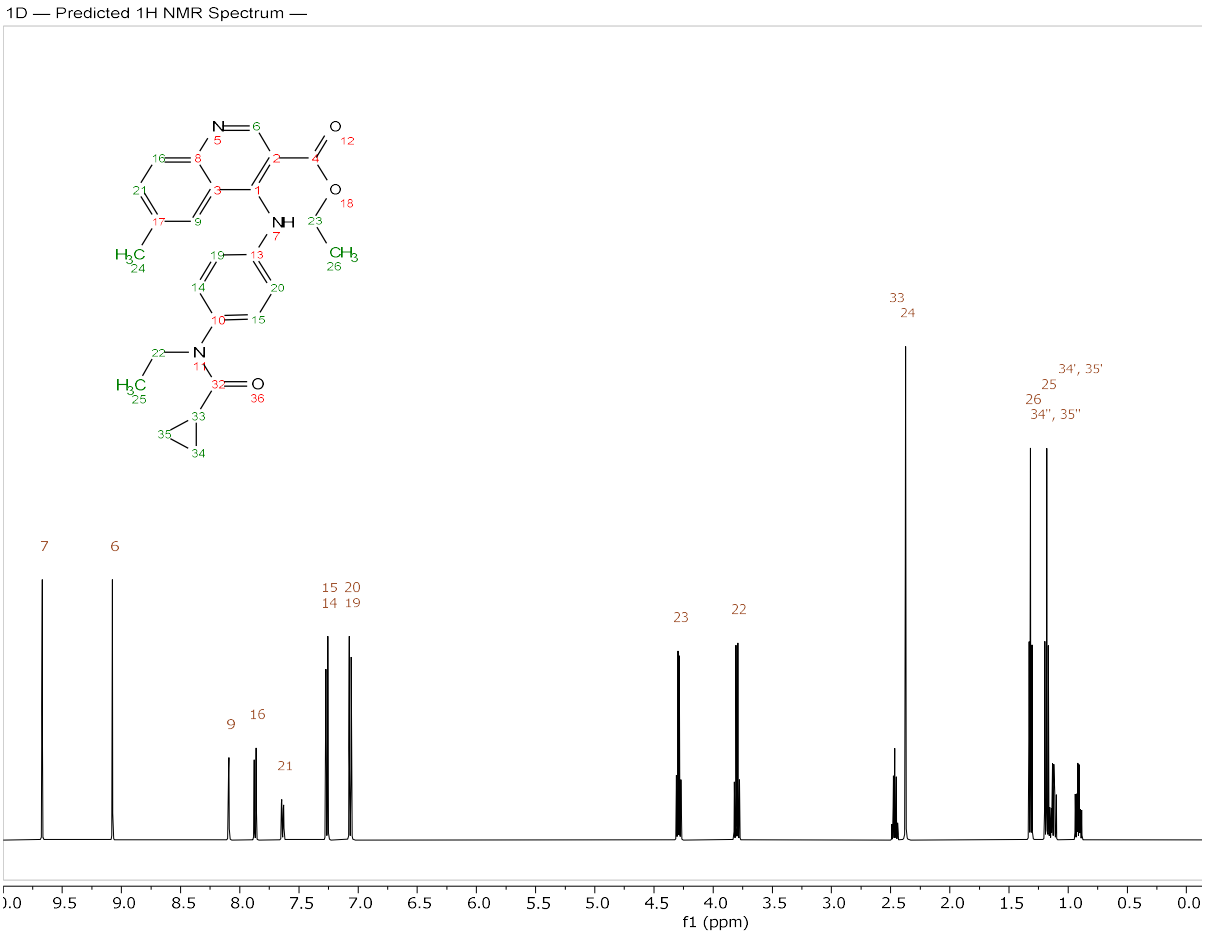

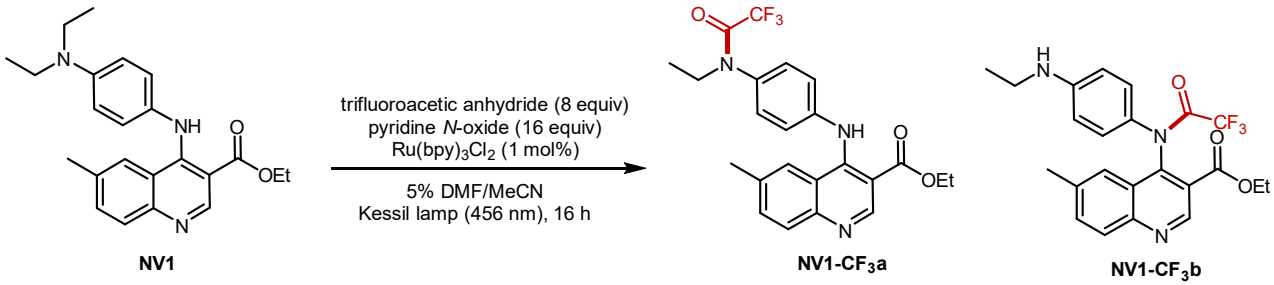

Ethyl 4-((4-(diethylamino)phenyl)amino)-6-methyl-2-(trifluoromethyl)quinoline-3-carboxylate (NV1-CF_3 a/b)

The reaction was run according to the 0.1 mmol scale-up procedure described above and was purified by mass-directed high performance liquid chromatography to afford the title compound (76 ug, 3%). **NV1-CF3 a**: 1H NMR (600 MHz, DMSO) δ 9.34 (s, 1H), 8.12 - 7.99 (m, 2H), 7.79 (d, J = 7.8 Hz, 1H), 7.29 (d, J = 8.5 Hz, 2H), 7.12 (d, J = 8.5 Hz, 2H), 4.41-4.49 (m, 4H), 2.07 (s, 3H), 1.35 (t, J = 7.1 Hz, 3H), 1.10 (t, J = 7.2 Hz, 3H).

NV1-CF_3 b 1H NMR (600 MHz, DMSO) δ 9.26 (s, 1H), 8.20 (s, 1H), 8.12 - 7.99 (m, 3H), 7.80 (d, J = 7.8 Hz, 1H), 6.48 (d, J = 8.9 Hz, 2H), 4.41 (m, 2H), 3.00 - 2.98 (m, 2H), 2.07 (s, 3H), 1.28 (t, J = 7.1 Hz, 3H), 1.10 (t, J = 7.2 Hz, 3H).

Waters SQ2 single-quad MS: m/z+ 446.3

NV1 CF3 (ROBINRI1-012-EXP045-001b)

m/z+ 446.3

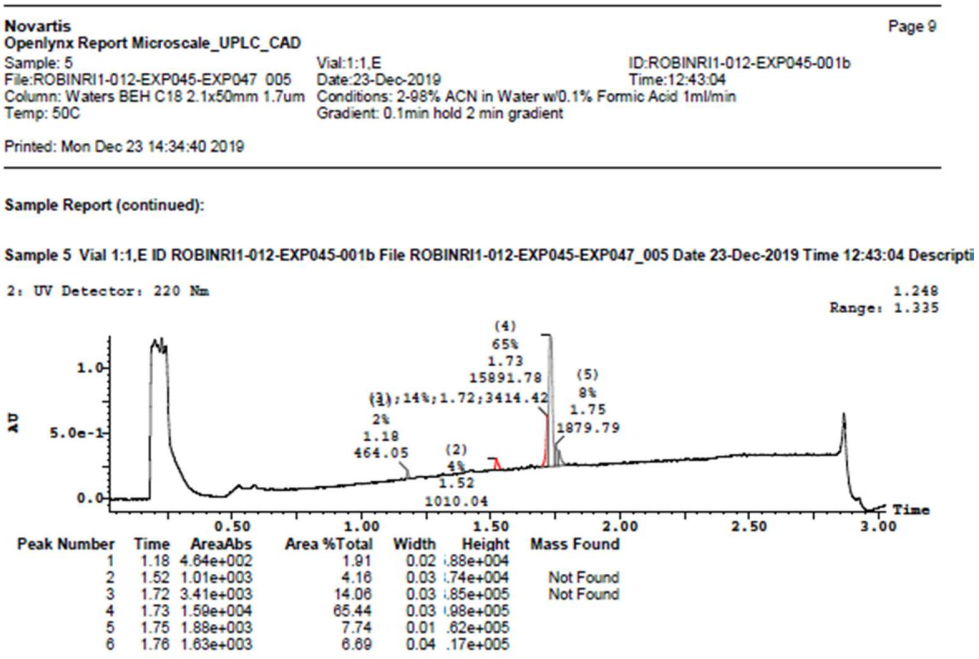

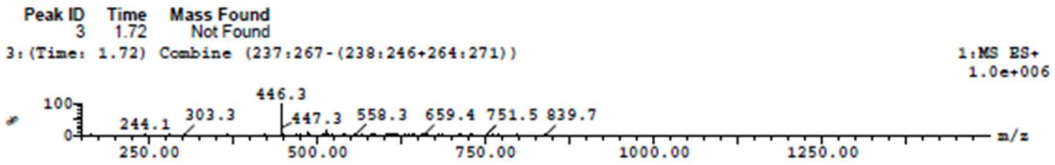

NV1-CF3 a/b predicted spectra: 2 isomer mixture (~1 : 1)

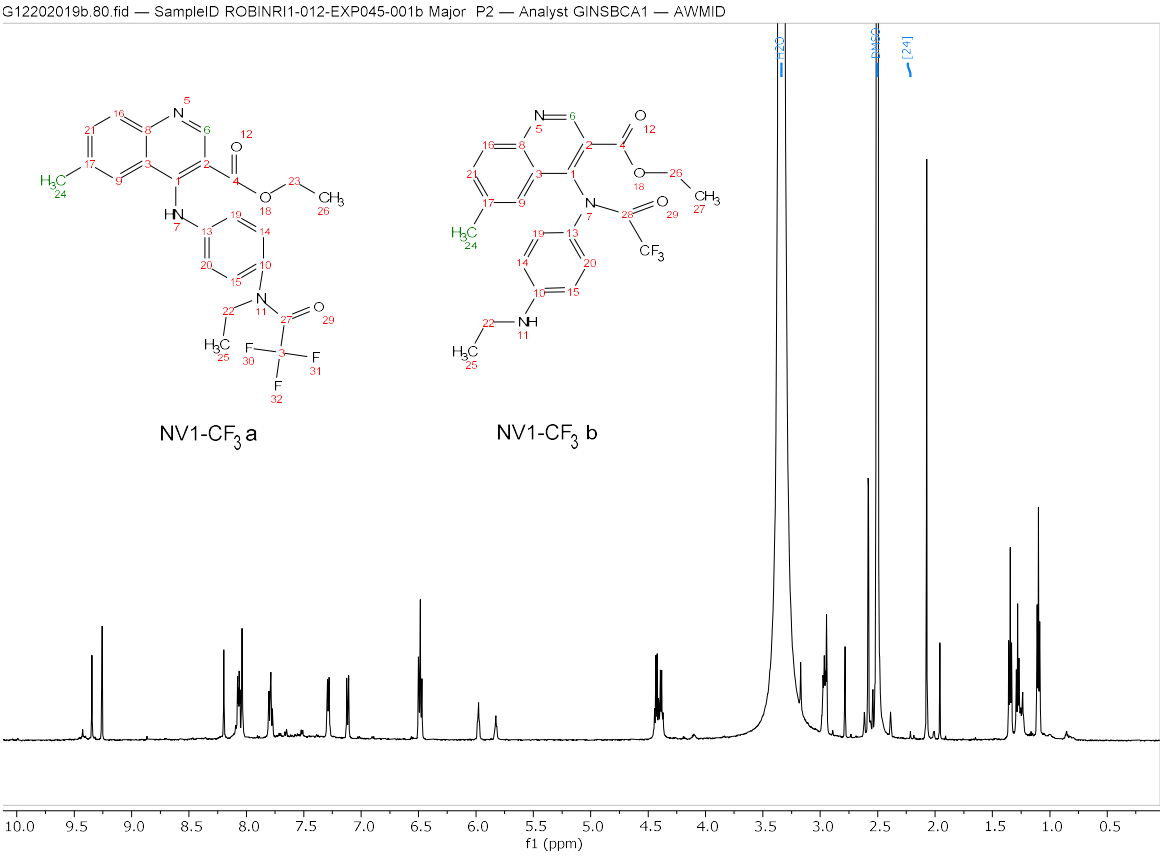

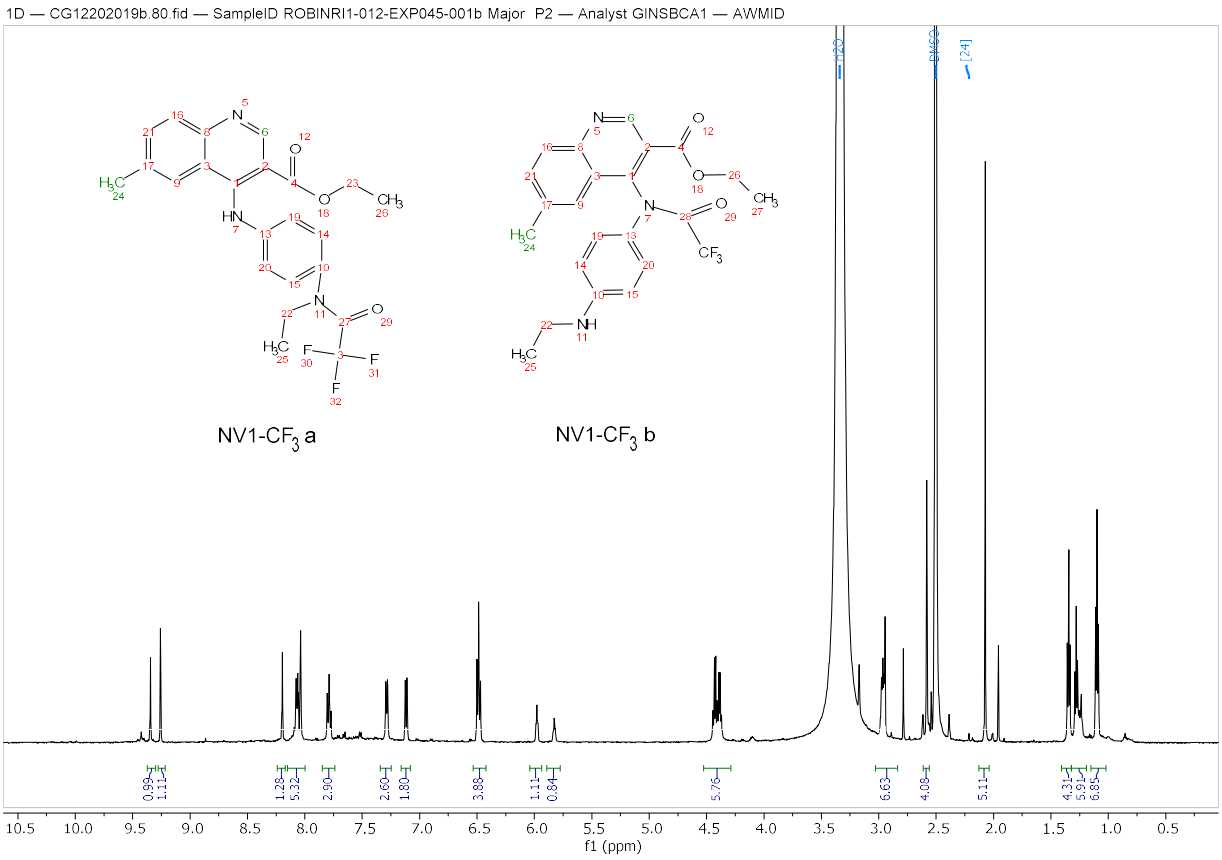
1D — CG12202019b.80.fid — SampleID ROBINRI1-012-EXP045-001b Major P2 — Analyst GINSBCA1 — AWMID
NV1-CF3 a
NV1-CF3 b
f1 (ppm)

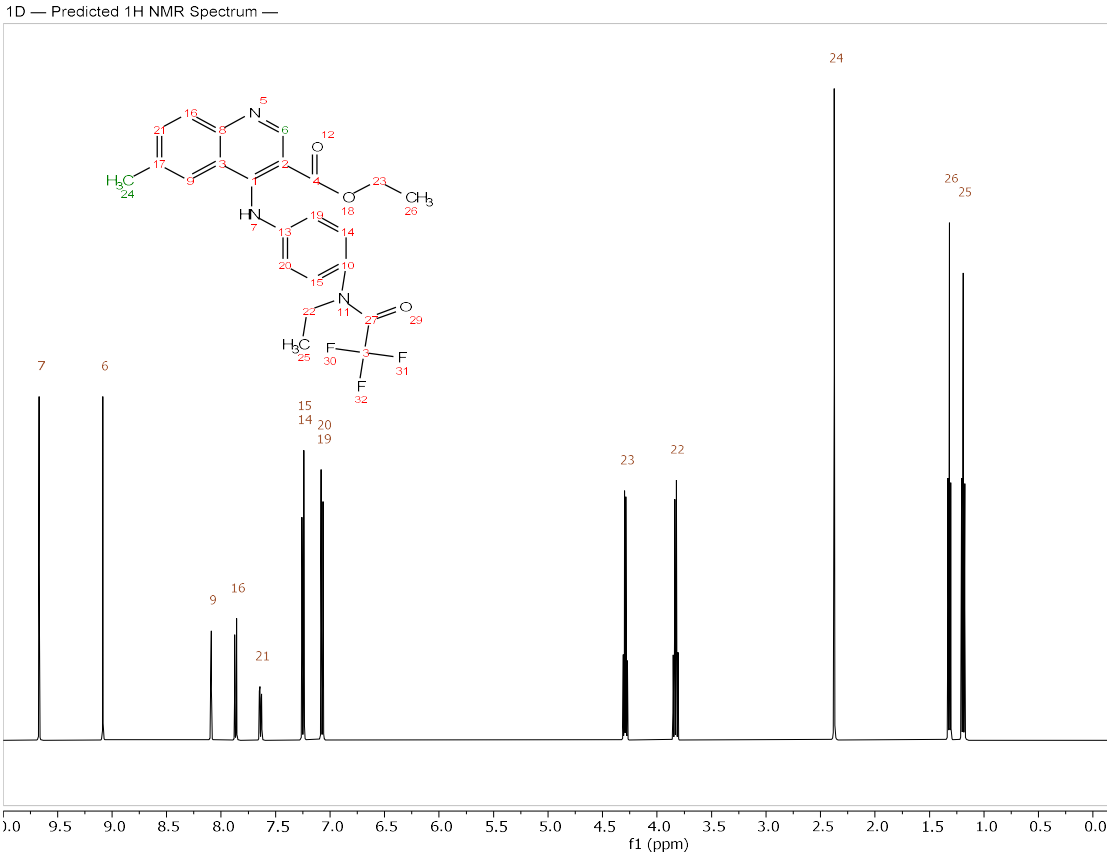
1D — Predicted 1H NMR Spectrum —
f1 (ppm)

1D — Predicted 1H NMR Spectrum —

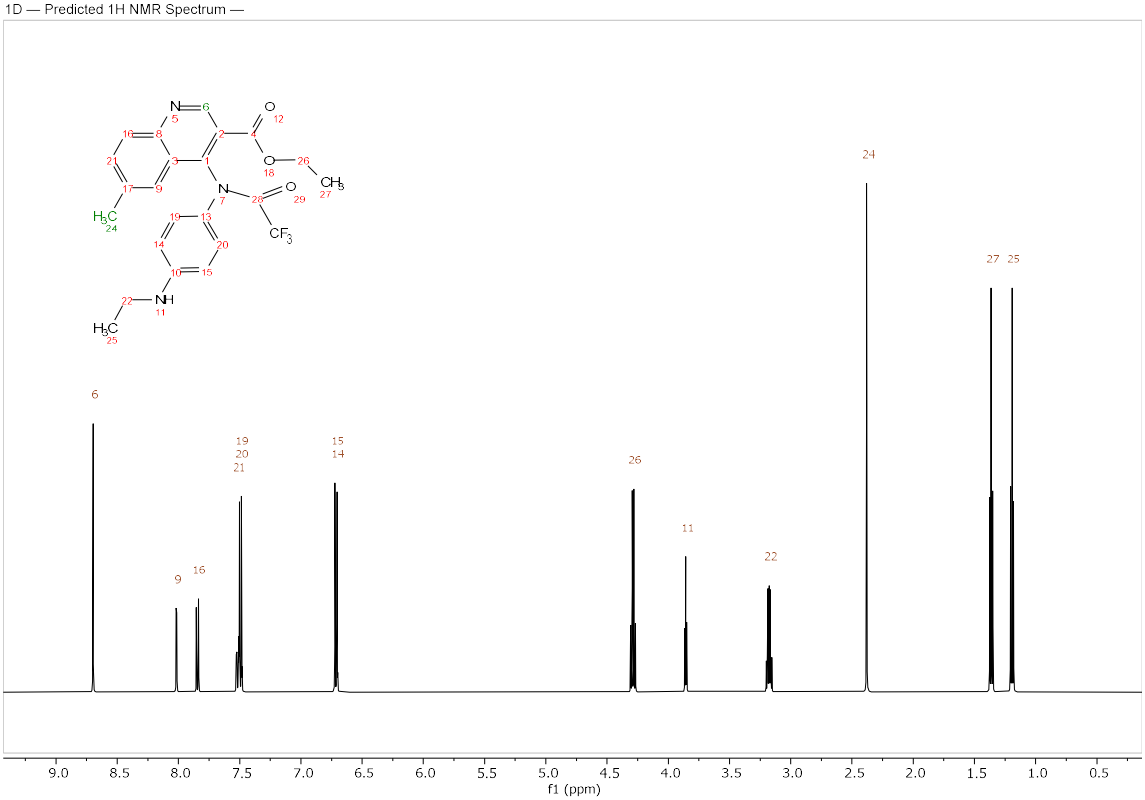

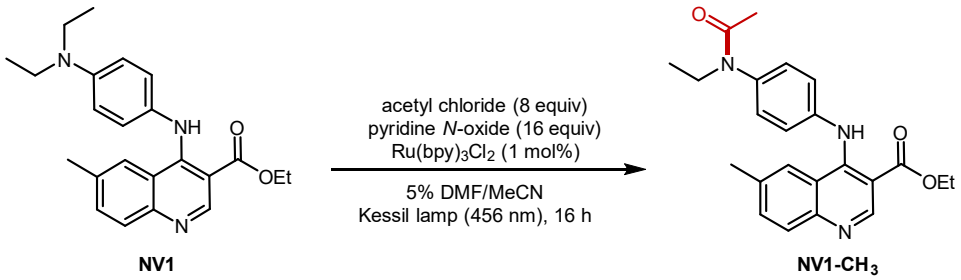

Ethyl 4-((4-(diethylamino)phenyl)amino)-2,6-dimethylquinoline-3-carboxylate (NV1-CH_3)
The reaction was run according to the 0.1 mmol scale-up procedure described above and was purified by mass-directed high performance liquid chromatography to afford the title compound (119 ug, 4%). ^{1}H NMR (600 MHz, DMSO) δ 9.66 (s, 1H), 8.87 (s, 1H), 7.90 – 7.82 (m, 3H), 7.63 (dd, *J* = 8.5, 1.9 Hz, 1H), 7.20 (d, *J* = 8.3 Hz, 2H), 7.09 (d, *J* = 8.4 Hz, 2H), 4.01 (q, *J* = 7.1 Hz, 2H), 3.61 (q, *J* = 7.2 Hz, 2H), 2.38 (s, 3H), 1.75 (s, 3H), 1.15 (t, *J* = 7.2 Hz, 3H), 1.01 (t, *J* = 7.2 Hz, 3H).
Waters SQ2 single-quad MS: m/z+ 392.3

NV1-Me/NV1-CH3 (ROBINRI1-012-EXP046-001)

m/z+ 392.3

Novartis Page 46
Openlynx Report Microscale_UPLC_CAD
Sample: 25 Vial:1:4,A ID:ROBINRI1-012-EXP046-001
File:ROBINRI1-012-EXP045-EXP047_025 Date:23-Dec-2019 Time:14:02:54
Column: Waters BEH C18 2.1x50mm 1.7um Conditions: 2-98% ACN in Water w/0.1% Formic Acid 1ml/min
Temp: 50C Gradient: 0.1min hold 2 min gradient

Printed: Mon Dec 23 14:34:40 2019

Sample Report (continued):

Sample 25 Vial 1:4,A ID ROBINRI1-012-EXP046-001 File ROBINRI1-012-EXP045-EXP047_025 Date 23-Dec-2019 Time 14:02:54 Description

2: UV Detector: 220 Nm 1.276
Range: 1.368

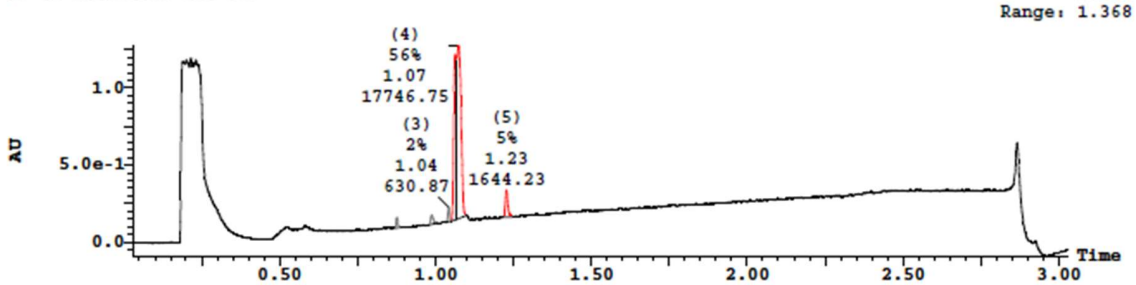

Peak Number	Time	AreaAbs	Area %Total	Width	Height	Mass Found
1	0.88	4.73e+002	1.49	0.02	.50e+004	
2	0.99	5.62e+002	1.78	0.02	.09e+004	
3	1.04	6.31e+002	1.99	0.02	.92e+004	
4	1.06	1.06e+004	33.49	0.02	.07e+006	Not Found
4	1.07	1.77e+004	56.06	0.03	.12e+006	Not Found
5	1.23	1.64e+003	5.19	0.03	.77e+005	Not Found

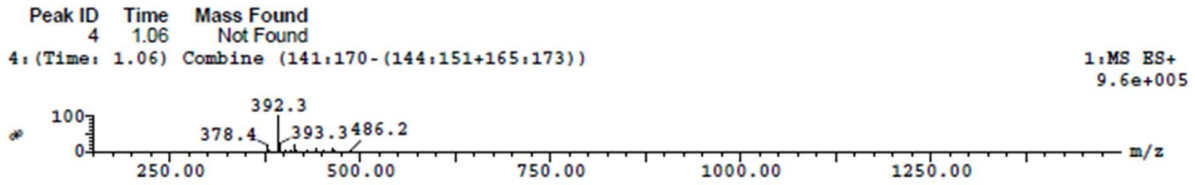
Peak ID Time Mass Found
4 1.06 Not Found
4:(Time: 1.06) Combine (141:170-(144:151+165:173))
1:MS ES+
9.6e+005
100
0
392.3
378.4
393.3
486.2
250.00
500.00
750.00
1000.00
1250.00
m/z

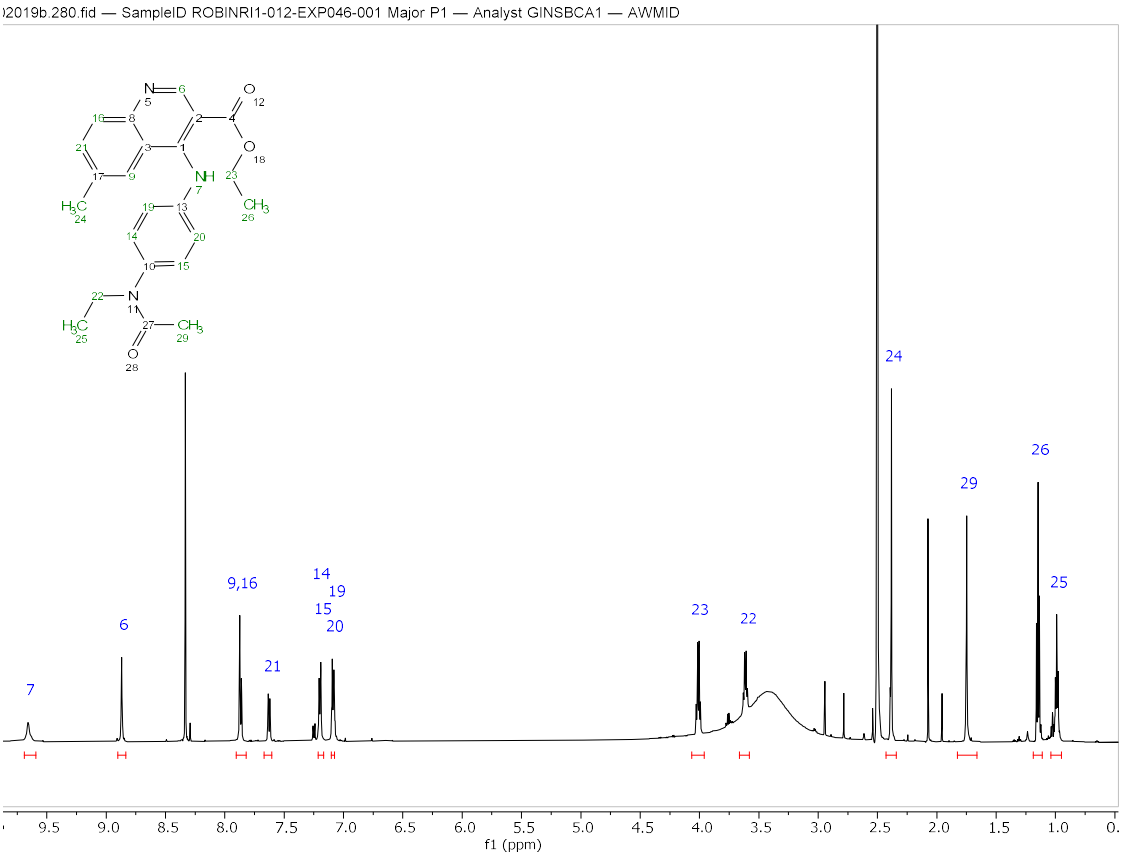
)2019b.280.fid — SampleID ROBINRI1-012-EXP046-001 Major P1 — Analyst GINSBCA1 — AWMID
7
6
9,16
21
14
19
15
20
23
22
24
29
26
25
f1 (ppm)

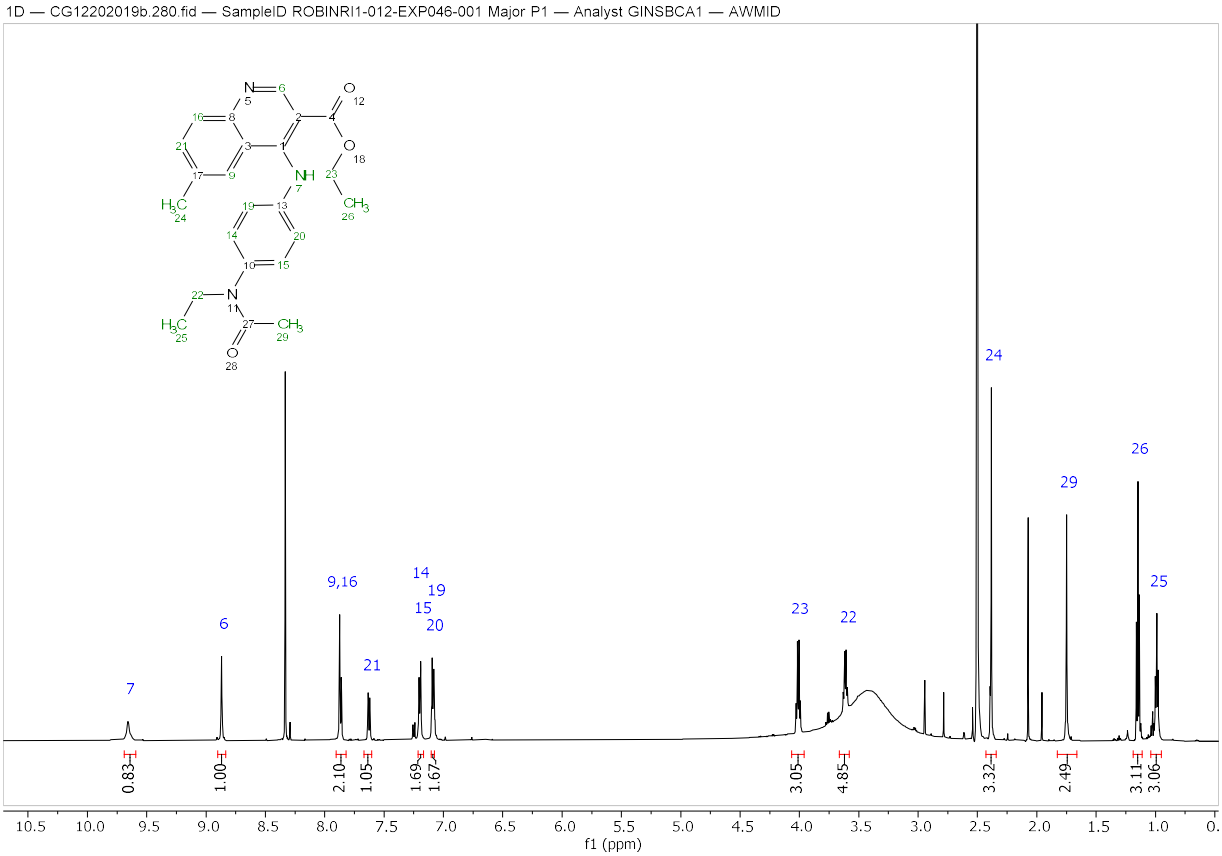
1D — CG12202019b.280.fid — SampleID ROBINRI1-012-EXP046-001 Major P1 — Analyst GINSBCA1 — AWMID
7
6
9,16
21
14
19
15
20
23
22
24
29
26
25
0.83
1.00
2.10
1.05
1.69
1.67
3.05
4.85
3.32
2.49
3.11
3.06
f1 (ppm)

1D — Predicted 1H NMR Spectrum —

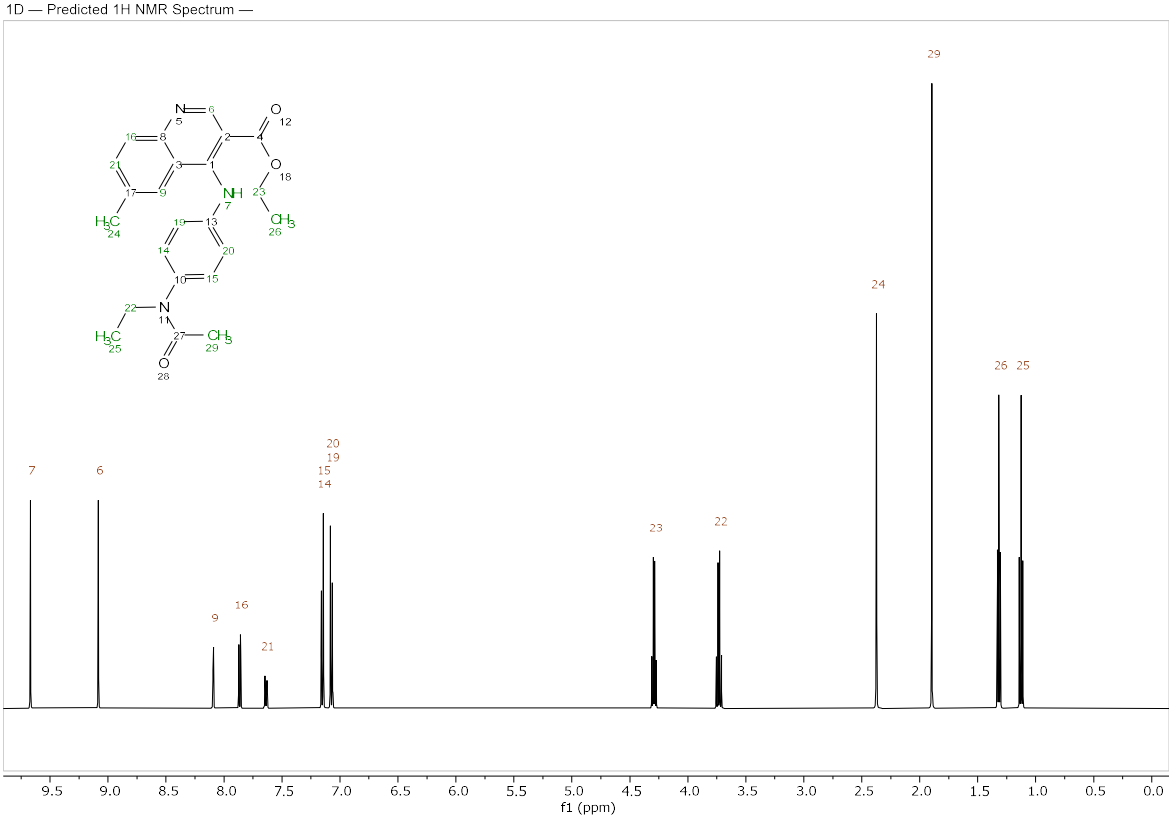

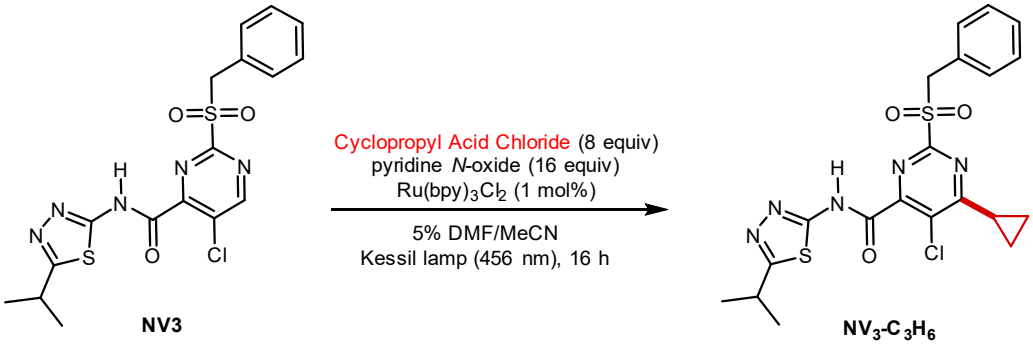

2-(Benzylsulfonyl)-5-chloro-6-cyclopropyl-N-(5-isopropyl-1,3,4-thiadiazol-2-yl)pyrimidine-4-carboxamide (NV3-C_3H_5)

The reaction was run according to the 0.1 mmol scale-up procedure described above and was purified by mass-directed high performance liquid chromatography to afford the title compound (285 ug, 11%). ^{1}H NMR (600 MHz, DMSO-d_6) δ 13.59 (s, 1H), 7.48 – 7.33 (m, 5H), 5.03 (s, 2H), 3.50-3.40 (m, 1H), 2.77-2.70 (m, 1H), 1.49 – 1.33 (m, 8H), 1.34-1.21 (m, 2H)., 6H). Waters SQ2 single-quad MS: m/z+ 478.3 [M+H]+

NV3-C3H5 (ROBINRI1-012-EXP047-003)

m/z+ 478.3

Novartis
Openlynx Report Microscale_UPLC_CAD
Page 44

Sample: 24
File:ROBINRI1-012-EXP045-EXP047_024
Column: Waters BEH C18 2.1x50mm 1.7um
Temp: 50C
Vial:1:3,H
Date:23-Dec-2019
Conditions: 2-98% ACN in Water w/0.1% Formic Acid 1ml/min
Gradient: 0.1min hold 2 min gradient
ID:ROBINRI1-012-EXP047-003
Time:13:58:55

Printed: Mon Dec 23 14:34:40 2019

Sample Report (continued):

Sample 24 Vial 1:3,H ID ROBINRI1-012-EXP047-003 File ROBINRI1-012-EXP045-EXP047_024 Date 23-Dec-2019 Time 13:58:55 Descriptio

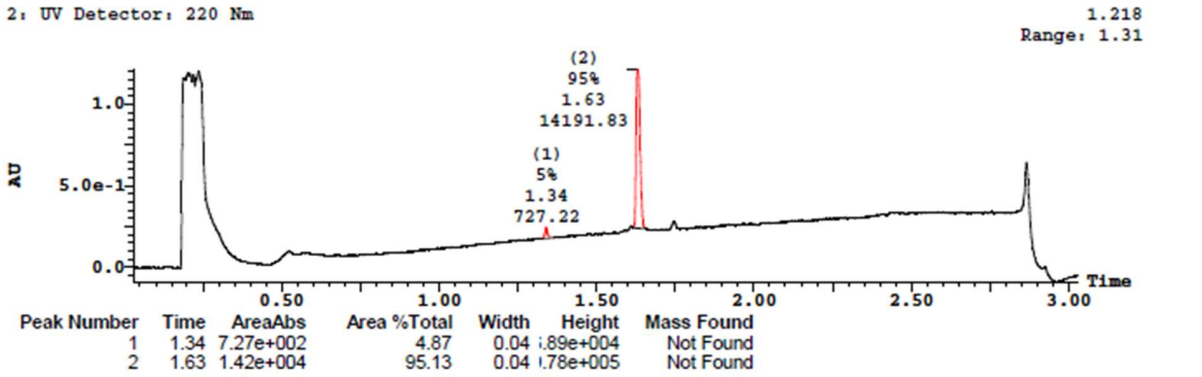

Peak Number	Time	AreaAbs	Area %Total	Width	Height	Mass Found
1	1.34	7.27e+002	4.87	0.04	1.89e+004	Not Found
2	1.63	1.42e+004	95.13	0.04	1.78e+005	Not Found

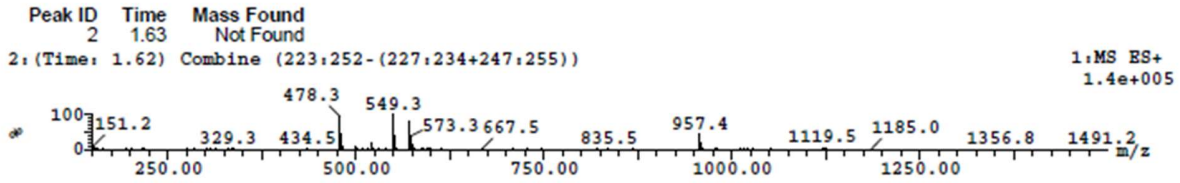
Peak ID Time Mass Found
2 1.63 Not Found
2:(Time: 1.62) Combine (223:252-(227:234+247:255))
1:MS ES+
1.4e+005
100
0
151.2
329.3
434.5
478.3
549.3
573.3
667.5
835.5
957.4
1119.5
1185.0
1356.8
1491.2
m/z
250.00
500.00
750.00
1000.00
1250.00

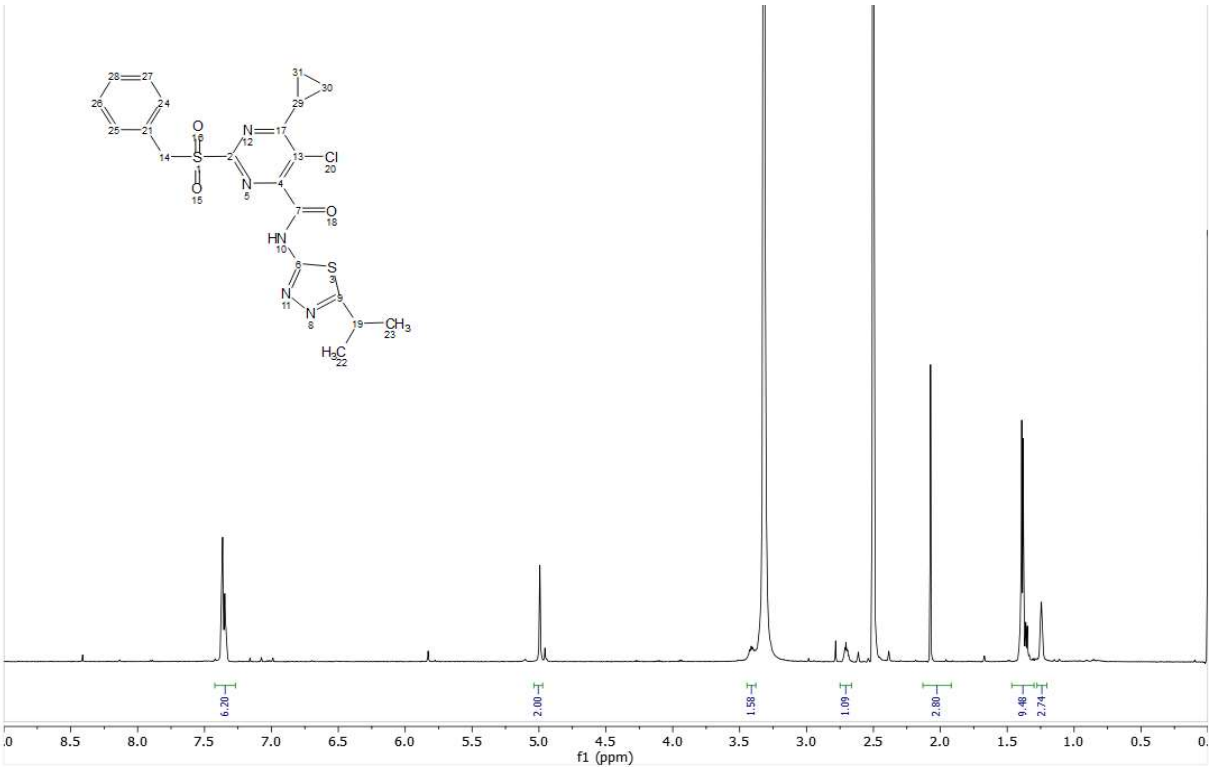
6.20
2.00
1.58
1.09
2.80
9.48
2.74
f1 (ppm)

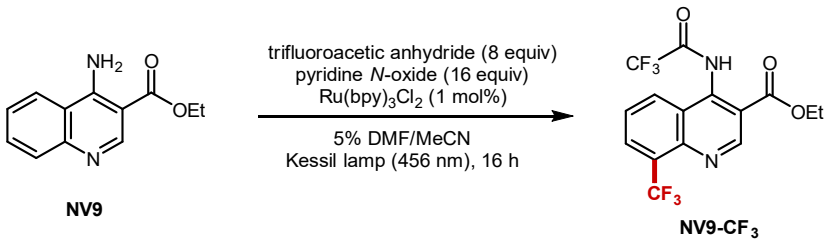

NV9 **NV9-CF_3**

Ethyl 4-(2,2,2-trifluoroacetamido)-8-(trifluoromethyl)quinoline-3-carboxylate (NV9-CF_3)
The reaction was run according to the 0.1 mmol scale-up procedure described above and was purified by mass-directed high performance liquid chromatography to afford the title compound (159 ug, 10%).^{1}H NMR (600 MHz, DMSO-d_6) δ 12.26 (br s, 1H; CF3CON*H*Ar), 9.37 (s, 1H), 8.43 (dd, *J* = 7.9 Hz, 1H), 8.39 (dd, *J* = 7.9 Hz, 1H), 7.93 (t, *J* = 8.0 Hz, 1H), 4.35 (q, *J* = 7.2 Hz, 2H, C*H*$_2$Me), 1.32 (t, *J* = 7.2 Hz, 3H, CH$_2$*Me*). Waters SQ2 single-quad MS: m/z+ 381.1

NV9-CF3 (ROBINRI1-012-EXP045-009)

m/z+ 381.1

Novartis Page 12
Openlynx Report Microscale_UPLC_CAD
Sample: 7 Vial:1:1,G ID:ROBINRI1-012-EXP045-009
File:ROBINRI1-012-EXP045-EXP047_007 Date:23-Dec-2019 Time:12:51:02
Column: Waters BEH C18 2.1x50mm 1.7um Conditions: 2-98% ACN in Water w/0.1% Formic Acid 1ml/min
Temp: 50C Gradient: 0.1min hold 2 min gradient

Printed: Mon Dec 23 14:34:40 2019

Sample Report (continued):

Sample 7 Vial 1:1,G ID ROBINRI1-012-EXP045-009 File ROBINRI1-012-EXP045-EXP047_007 Date 23-Dec-2019 Time 12:51:02 Description

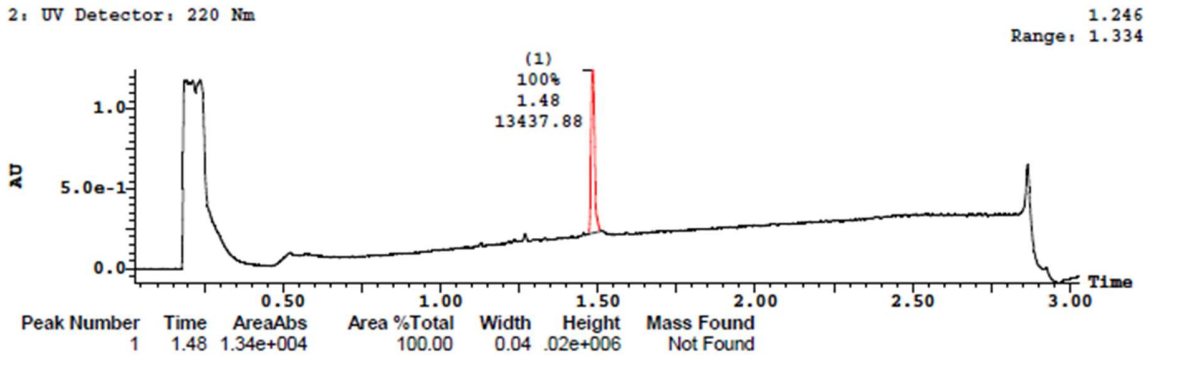

Peak Number	Time	AreaAbs	Area %Total	Width	Height	Mass Found
1	1.48	1.34e+004	100.00	0.04	.02e+006	Not Found

Peak ID	Time	Mass Found
1	1.48	Not Found

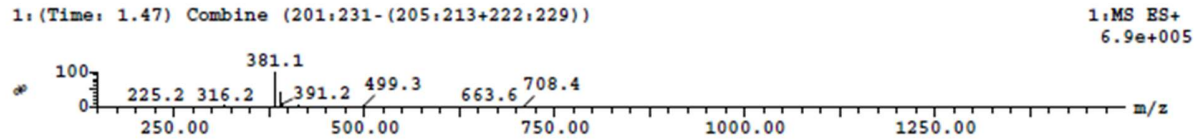

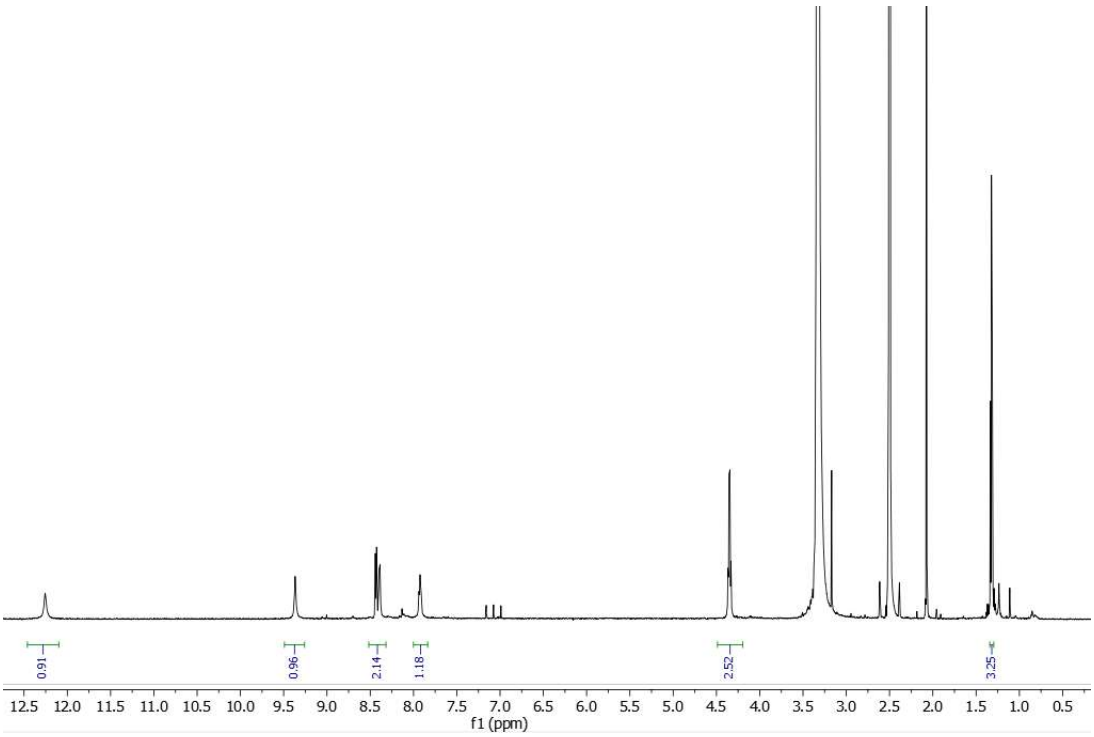

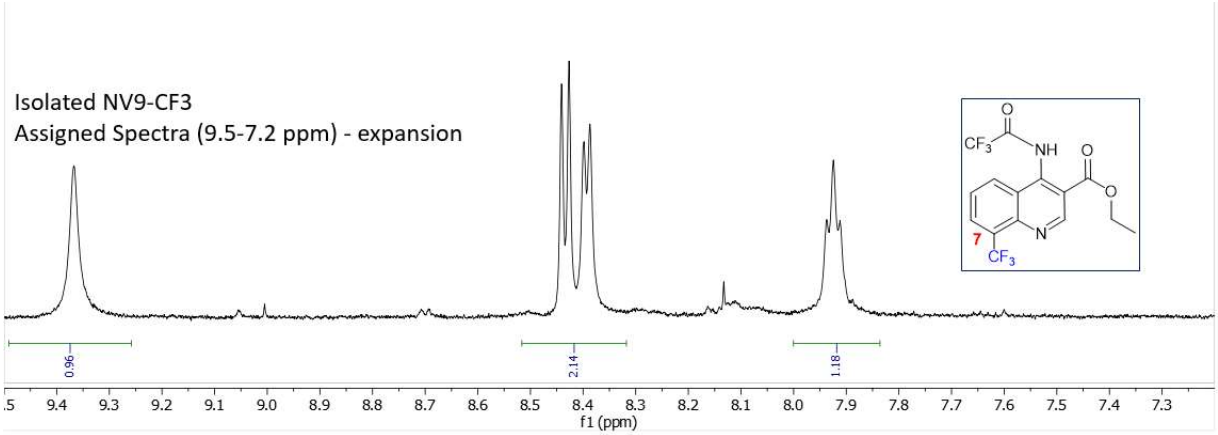

The structure of NV9-CF3 was assigned based on the predictions of chemical shifts and coupling multiplet patterns of all possible regioisomers.

Predicted NV9 CF3 isomers: Enabling Structure Assignment Matching

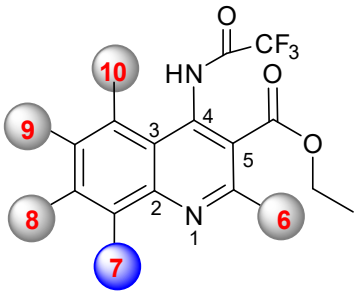

CF_3 (position)	Assignment	Predicted Spectra (showing region 9.5-7.2 ppm)
6	δ 8.01 (ddd, *J* = 7.3, 4.3, 1.5 Hz, 2H), 7.85 (td, *J* = 7.5, 1.6 Hz, 1H), 7.56 (td, *J* = 7.5, 1.5 Hz, 1H), 4.26 (q, *J* = 5.9 Hz, 2H), 1.33 (t, *J* = 5.9 Hz, 3H).	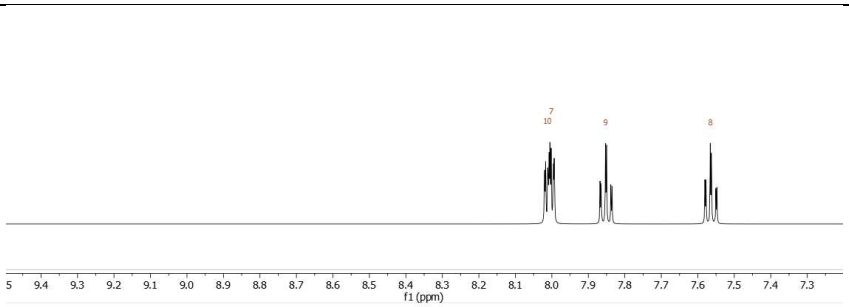
7 * **Closest Target Match**	δ 9.23 (s, 1H), 8.18 (dd, *J* = 7.5, 1.5 Hz, 1H), 8.03 (dd, *J* = 7.5, 1.5 Hz, 1H), 7.62 (t, *J* = 7.5 Hz, 1H), 4.28 (q, *J* = 5.9 Hz, 2H), 1.33 (t, *J* = 5.9 Hz, 3H).	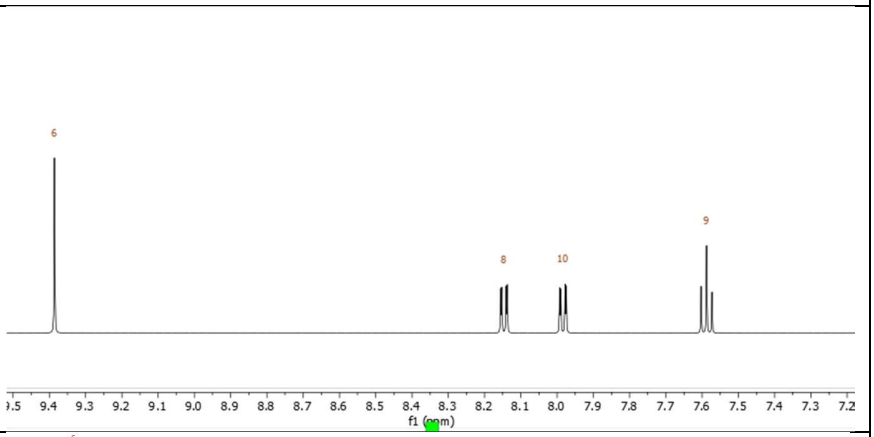
8	δ 9.30 (s, 1H), 8.33 (d, *J* = 7.6 Hz, 1H), 8.19 (d, *J* = 1.5 Hz, 1H), 7.64 (dd, *J* = 7.5, 1.5 Hz, 1H), 4.28 (q, *J* = 5.9 Hz, 2H), 1.33 (t, *J* = 5.9 Hz, 3H).	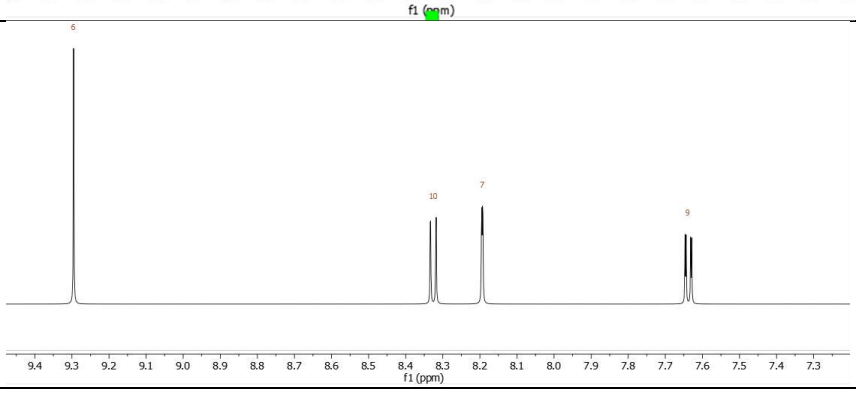

9	δ 9.36 (s, 1H), 8.59 (d, J = 1.6 Hz, 1H), 8.19 (d, J = 7.5 Hz, 1H), 8.01 (dd, J = 7.5, 1.5 Hz, 1H), 4.28 (q, J = 5.9 Hz, 2H), 1.33 (t, J = 5.9 Hz, 3H).	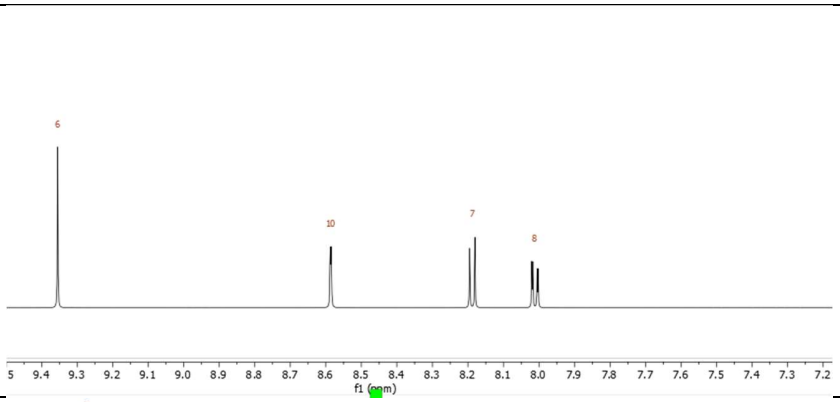
10	δ 9.27 (s, 1H), 8.02 (dd, *J* = 7.5, 1.5 Hz, 1H), 7.97 – 7.90 (m, 1H), 7.80 (dd, *J* = 7.5, 1.5 Hz, 1H), 4.28 (q, *J* = 5.9 Hz, 2H), 1.33 (t, *J* = 5.9 Hz, 3H).	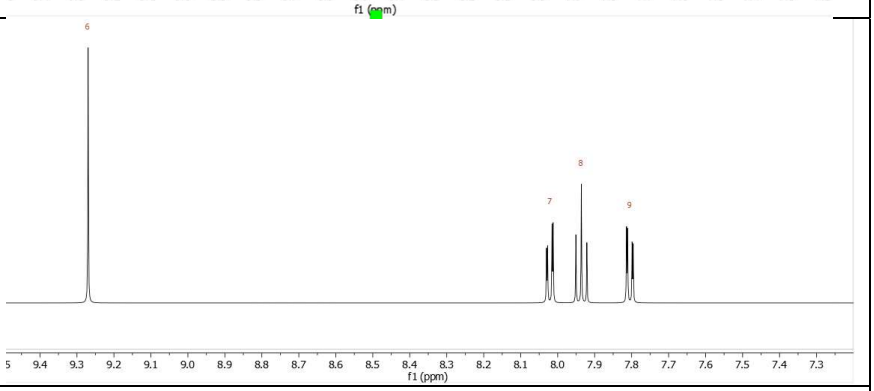

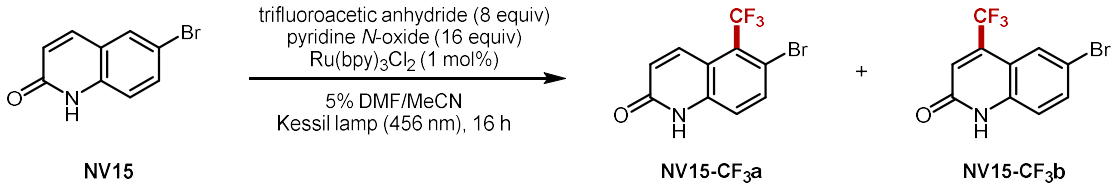

NV15 NV15-CF_3a NV15-CF_3b

6-bromo-5-(trifluoromethyl)quinolin-2(1H)-one (NV15-CF_3a)

The reaction was run according to the 0.1 mmol scale-up procedure described above and was purified by mass-directed high performance liquid chromatography to afford the title compound (159 ug); purity 88 %. Major Regio-isomer. ^{1}H NMR (600 MHz, DMSO-d_6) δ 12.24 (s, 1H), 8.09 (dd, *J* = 10.2, 2.0 Hz, 1H), 7.94 (d, *J* = 9.0 Hz, 1H), 7.50 (d, *J* = 9.0 Hz, 1H), 6.73 (dd, *J* = 10.2, 2.0 Hz, 1H). [Purity 90 % by NMR]. Waters SQ2 single-quad MS: m/z+ 292.0; 294.0 [M+H]+ 1:1 Br isotope Rt= 1.35 min.

Novartis Page 20
Openlynx Report Microscale_UPLC_CAD
Sample: 11 Vial:1:2,C ID:ROBINRI1-012-EXP045-015
File:ROBINRI1-012-EXP045-EXP047_011 Date:23-Dec-2019 Time:13:07:00
Column: Waters BEH C18 2.1x50mm 1.7um Conditions: 2-98% ACN in Water w/0.1% Formic Acid 1ml/min
Temp: 50C Gradient: 0.1min hold 2 min gradient

Printed: Mon Dec 23 14:34:40 2019

Sample Report (continued):

Sample 11 Vial 1:2,C ID ROBINRI1-012-EXP045-015 File ROBINRI1-012-EXP045-EXP047_011 Date 23-Dec-2019 Time 13:07:00 Descr

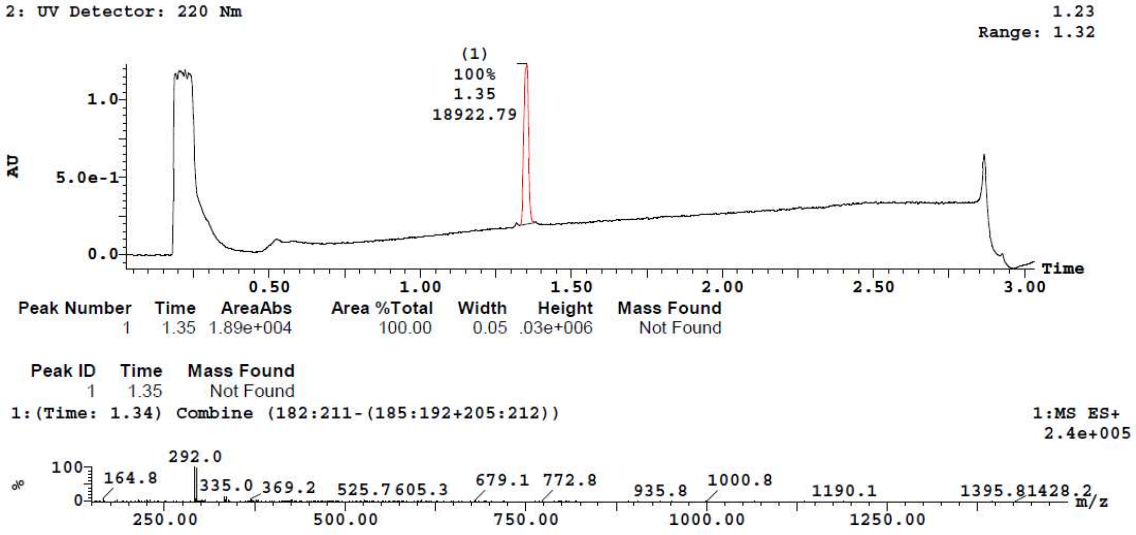

Peak Number	Time	AreaAbs	Area %Total	Width	Height	Mass Found
1	1.35	1.89e+004	100.00	0.05	.03e+006	Not Found

Peak ID	Time	Mass Found
1	1.35	Not Found

1D — CG12202019b.140.fid — SampleID ROBINRI1-012-EXP045-015 Major P1 — Analyst GINSBCA1 — AWMID

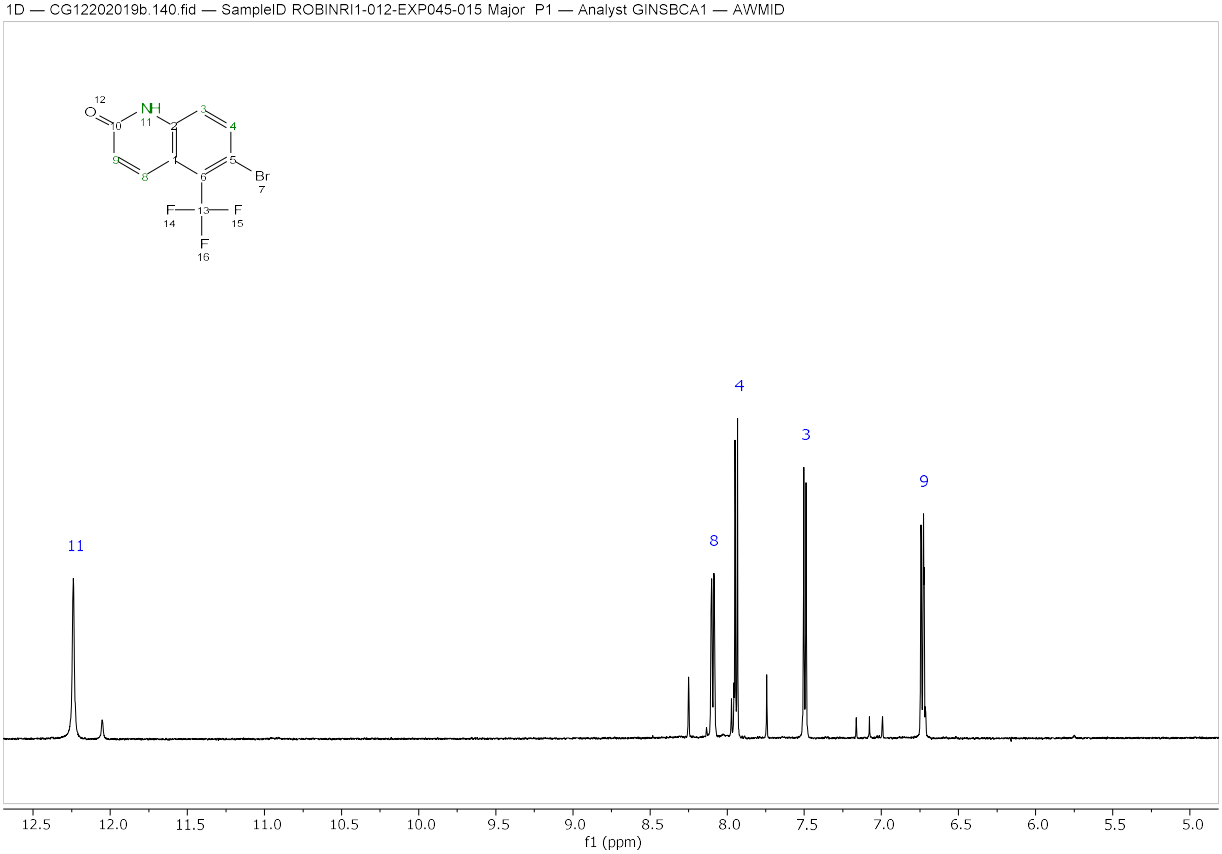

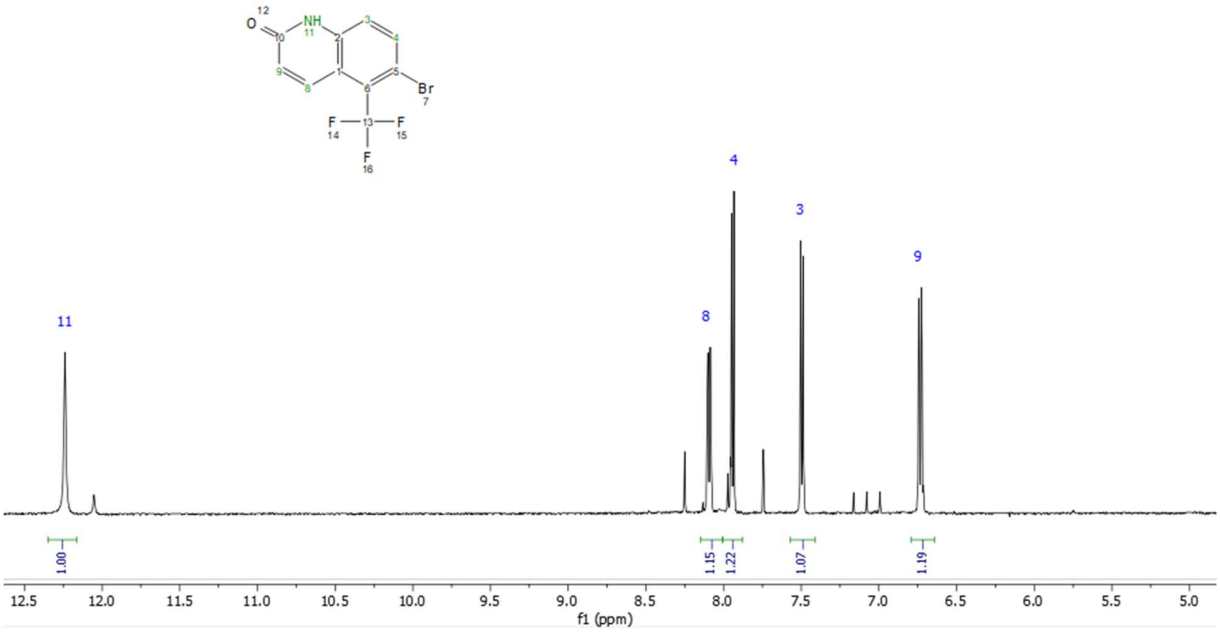

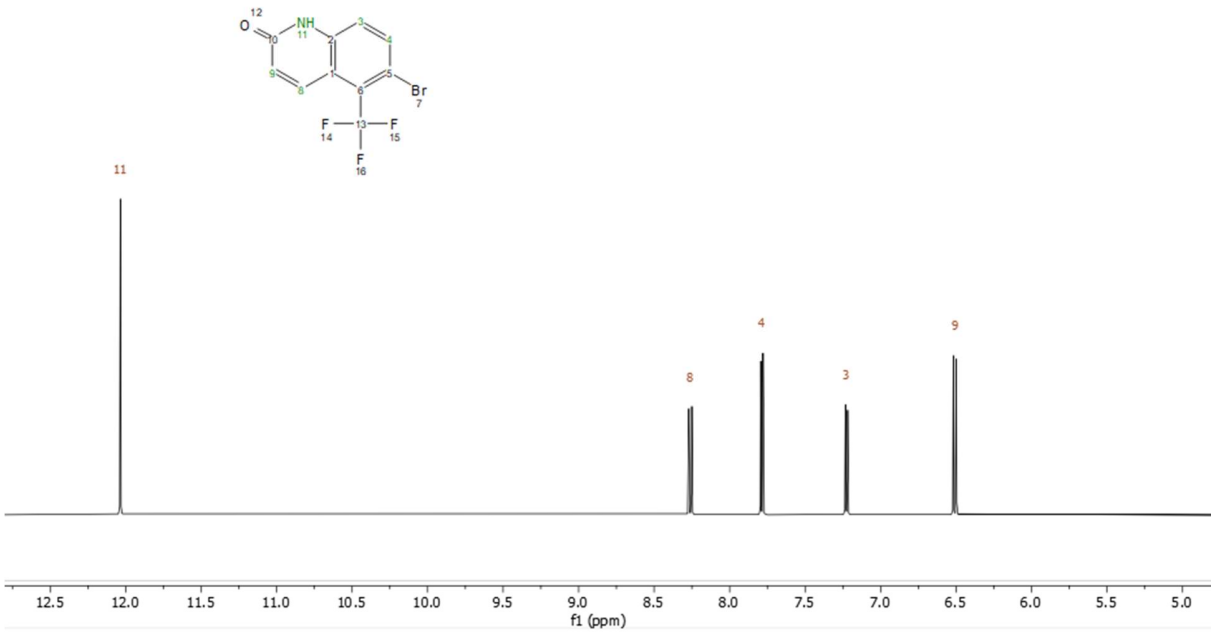

6-bromo-4-(trifluoromethyl)quinolin-2(1H)-one (NV15-CF3b) – Minor Isomer

The title compound was isolated as the minor product (23 ug) following separation from NV15-CF3b. ^{1}H NMR (600 MHz, DMSO-d_6) δ 12.46 (s, 1H), 7.86 – 7.81 (m, 1H), 7.77 – 7.72 (m, 1H), 7.40 (d, J = 8.8 Hz, 1H), 7.07 (s, 1H). Waters SQ2 single-quad MS: m/z+ 292.0; 294.0 [M+H]+ 1:1 Br isotope; Rt= 1.43 min.

Openlynx Report Microscale_UPLC_CAD

Sample: 13 Vial:1:2,E ID:ROBINRI1-012-EXP045-015
File:ROBINRI1-012-EXP045-EXP047_013 Date:23-Dec-2019 Time:13:14:59
Column: Waters BEH C18 2.1x50mm 1.7um Conditions: 2-98% ACN in Water w/0.1% Formic Acid 1ml/min
Temp: 50C Gradient: 0.1min hold 2 min gradient

Printed: Mon Dec 23 14:34:40 2019

Sample Report (continued):

Sample 13 Vial 1:2,E ID ROBINRI1-012-EXP045-015 File ROBINRI1-012-EXP045-EXP047_013 Date 23-Dec-2019 Time 13:14:59 Descripti

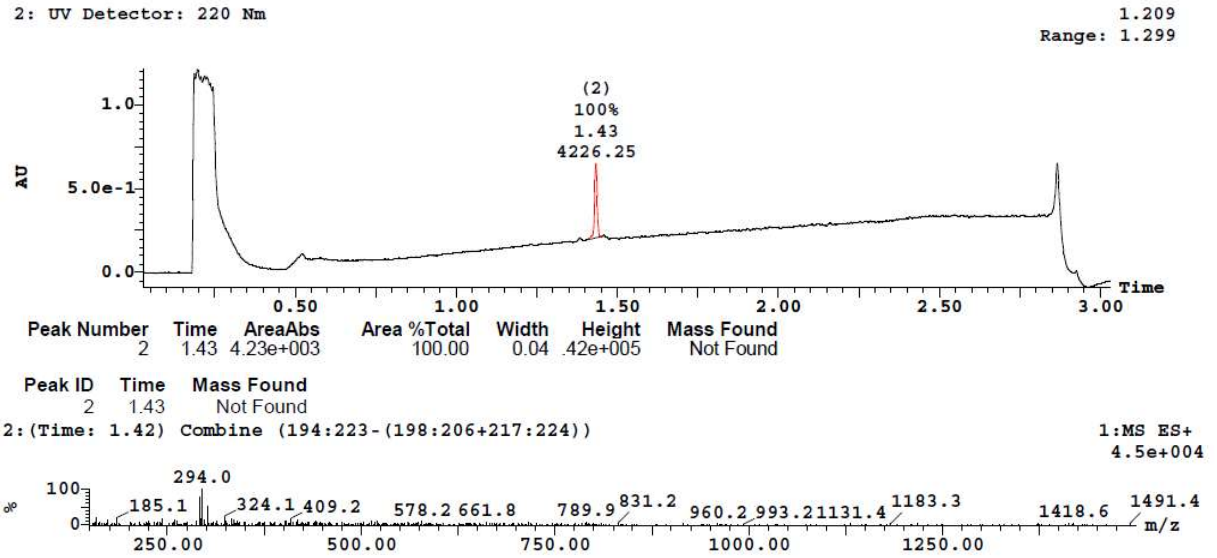

Peak Number	Time	AreaAbs	Area %Total	Width	Height	Mass Found
2	1.43	4.23e+003	100.00	0.04	.42e+005	Not Found

Peak ID	Time	Mass Found
2	1.43	Not Found

(NV15-CF3b) - minor isolated regio-isomer; not assayed due to insufficient quantity for 10 mM stock (23 ug):-

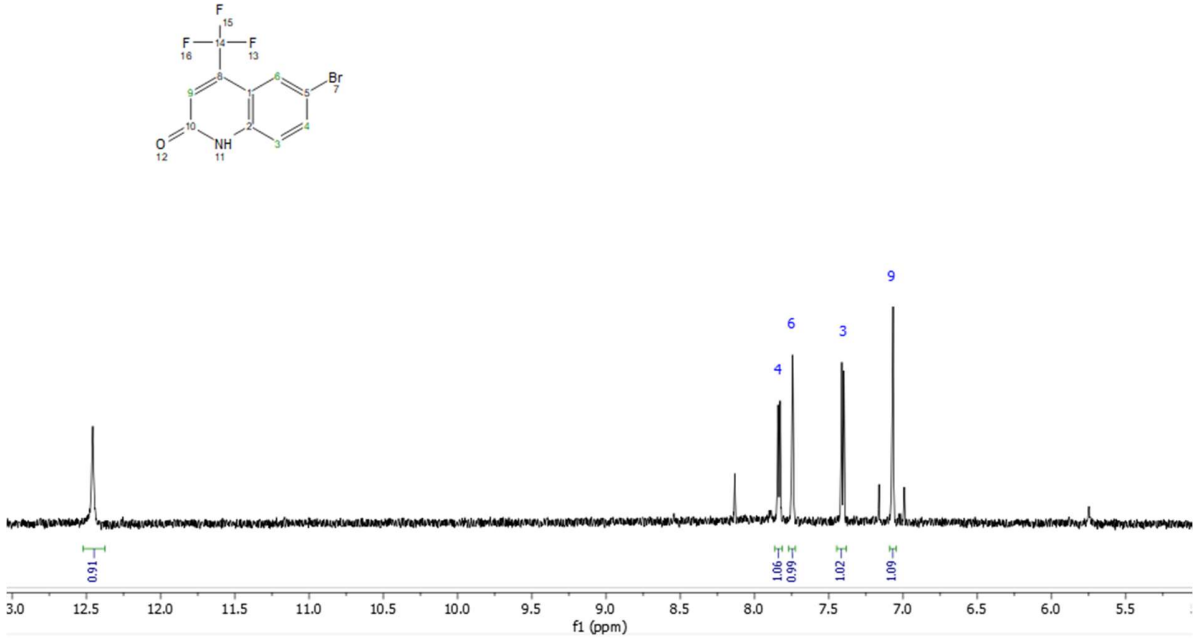

Comparison **(NV15-CF3b)** to genuine sample[68] [CAS 328955-61-9] below; purchased from ***AmBeed A912781-003*** confirmed assignment.

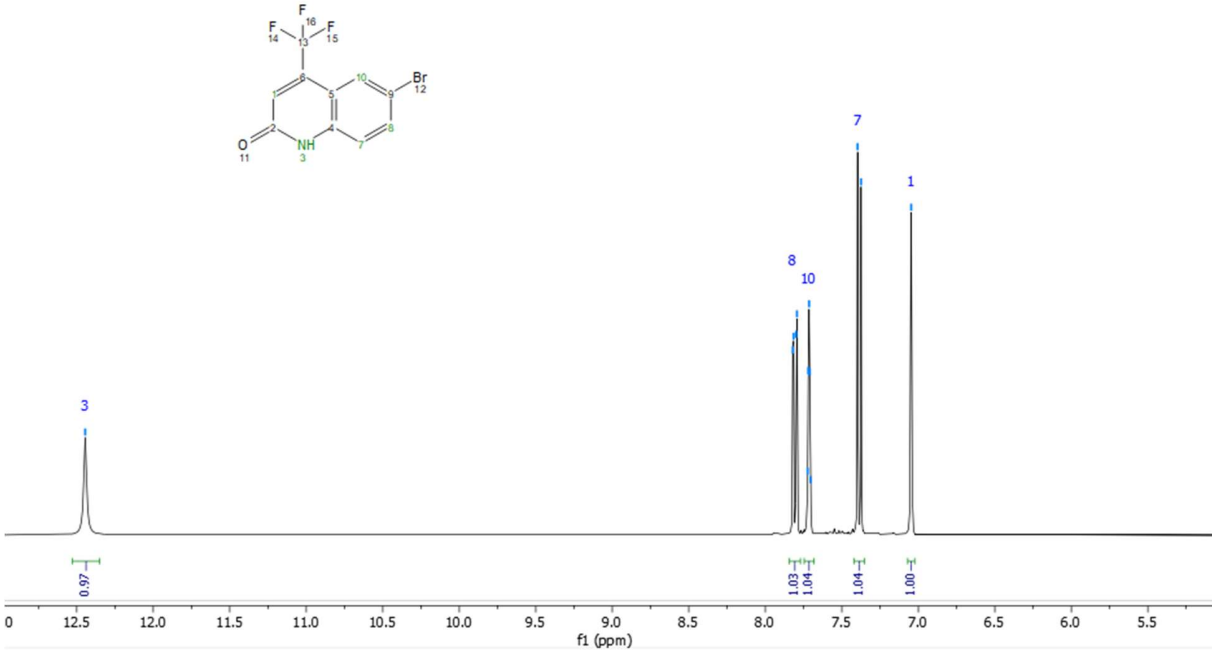

(68) Wlodarczyk, N.; Simenel, C.; Delepierre, M.; Barale, J. C. *Synthesis* **2011**, *6*, 934-942.

Increasing Analysis Throughput

While the original throughput established was determined by the duty cycle of 170 ms necessary to perform full MS scans, the MS-MS method established for trifluoromethylated caffeine required only 40 ms. This MS-MS method was applied for the observation of droplets at even higher throughputs. To achieve higher throughputs while maintaining the integrity of the droplet samples, we focused on the optimization of two system components: the internal diameter (i.d.) of the fused silica nESI emitter and the size of the droplets (Figure S20). Our original caffeine trifluoromethylation nESI-MS-MS analysis conditions involved the use of a 75 μm i.d. emitter capillary to form 8 nL droplets with 12 nL PFD segmentation, flowed at 800 nL/min to give a throughput of 0.67 droplets/s. Any increases to flow rate caused breakage of droplets inside of the 75 μm emitter; however, we discovered that increasing the capillary i.d. to 100 μm allowed for stable flow of droplets at higher flow rates. Stable droplet transfer through the capillary at 1500 nL/min flow was now possible, increasing analysis throughput to 1.3 droplets/s. To further increase throughput, the volumes of the droplets and PFD spacing were decreased to 3 nL and 4 nL, respectively. By combining reduced sample volumes with higher flow rates, analysis throughput was successfully increased to 2.9 droplets/s. For reference, triplicate MS analysis of a 384 microwell plate could be achieved in under 7 minutes.

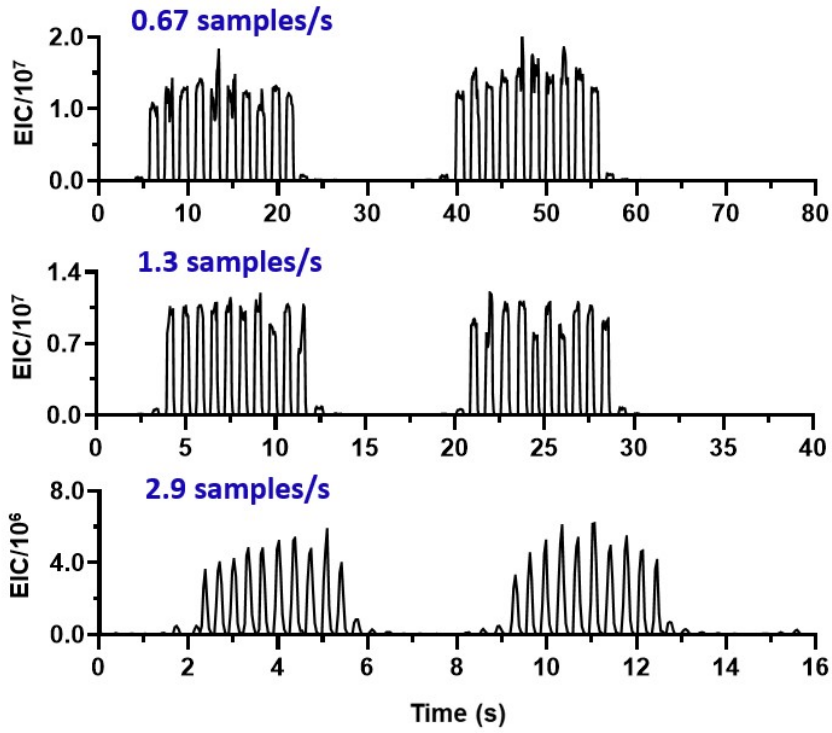

Figure S19. Efforts to increase throughput. Traces represent the MS-MS detection of trifluormethylated caffeine (m/z = 263→191). Samples were formatted into repeating 10x10 units of samples (50 μm) and blanks (Top) The use of 75 μm i.d. capillary emitter, 8 nL droplets, and 12 nL PFD spacing was capable of stable analysis at 800 nL/min flow and 0.67 droplet/s throughput. (Middle) The use of 100 μm i.d. capillary emitter, 8 nL droplets, and 12 nL PFD spacing was capable of stable analysis at 1500 nL/min flow and 1.3

droplet/s throughput. (Bottom) The use of 100 µm i.d. capillary emitter, 4 nL droplets, and 3 nL PFD spacing was capable of stable analysis at 1500 nL/min flow and 2.9 droplet/s throughput.